PROBABILITY OF WELLBORE FAILURE AND ITS PREDICTION USING MACHINE LEARNING

A thesis presented to the Department of Petroleum Engineering African University of Science and Technology, Abuja

In partial fulfillment of the requirements for the degree of

MASTER OF SCIENCE

By

KOLADE, EMMANUEL BAMIDELE

Supervised by

Dr. Xingru Wu

African University of Science and Technology www.aust.edu.ng

P.M.B 681, Garki, Abuja F.C.T Nigeria

June, 2019

Certification

This is to certify that the thesis titled "*Probability of Wellbore Failure and its Prediction Using Machine Learning*" submitted to the school of postgraduate studies, African University of Science and Technology (AUST), Abuja, Nigeria for the award of the Master's degree is a record of original research carried out by *Kolade, Emmanuel Bamidele in the Department of Petroleum Engineering*

PROBABILITY OF WELLBORE FAILURE AND ITS PREDICTION USING MACHINE LEARNING

By

Kolade, Emmanuel Bamidele

A THESIS APPROVED BY THE PETROLEUM ENGINEERING DEPARTMENT

RECOMMENDED: ……

Supervisor; Dr. Xingru WU

……

Committee Member; Prof. David Ogbe

Head, Department of Petroleum Engineering

APPROVED: …….....

Chief Academic Officer

…….....

Date

ABSTRACT

Kolade, Emmanuel Bamidele: Probability of Wellbore Failure and its Prediction Using Machine Learning

(Under the direction of Xingru Wu)

Wellbore instability (WI) is one of the major challenges experienced during drilling operations costing the oil and gas industry over $1 billion yearly. During the drilling, borehole breakout and drilling induced fractures are the two main instability problems which may lead to stuck pipe, sidetracking and loss of circulation. Due to large uncertainties of subsurface data such as rock Poisson ratio and permeability and impact of drilling fluid dynamics and density, the prediction of wellbore failure probability poses a challenge. Bayesian analyses provide a great framework for this type of probabilistic analysis. In this research, two common failure criterion-Mogi-Coulomb and Mohr-Coulomb failure criteria were applied to synthetic data. Subsequently, Gaussian Naïve Bayes (GNB) algorithm was applied to the outcome to probabilistically predict wellbore failure, and it is shown that GNB was able to predict wellbore failure with 86.7% and 67.3% accuracy respectively for the Mogi-Coulomb and Mohr-Coulomb model.

Keywords: *Wellbore Failure, Machine Learning, Bayesian, Prediction*

ACKNOWLEDGMENTS

Special thanks to my supervisor, Dr. Xingru Wu, for providing me with the opportunity and means to grow and thrive under his guidance. He has inspired me with his success story and disposition to science and life generally. He has taught me that limits are self- imposed, and should always be challenged. He has provided me with strong leadership and direction in the bid to achieve a milestone in my research quest and scientific development.

My profound gratitude to Prof. Ogbe for the measures he put in place to ensure I was always tapping into my full potential. I also would like to thank Dr. Igbokoyi for his time, guidance and candid advice as my HOD. Thank you so much Profs.

I acknowledge AfDB for giving me the opportunity, through a scholarship, to be part of this petroleum engineering program. I thank every faculty of the petroleum engineering department for professional experience in training me as a petroleum engineer. I appreciate every staff, my dear friends and colleagues at the African University of Science and Technology, Abuja for your part in making my study a comfortable and meaningful one.

To my amiable friends, Helena, Hanson, Bose, Abu, Francis, Fawziyah, the rest of my classmates and all AUST SPE members, thanks for your understanding, cooperation, support, and encouragement. I really had a nice and memorable time with you guys.

DEDICATION

I dedicate this work to Almighty God for giving me the grace to complete it and to my loving parents for always being by me.

TABLE OF CONTENTS

LIST OF TABLES

LIST OF FIGURES

CHAPTER 1
INTRODUCTION

1.1 BACKGROUND

Wellbore instability (WI) is one of the major challenges experienced during drilling operations. It is estimated that the yearly non-productive time (NPT) identified with wellbore instability costs the oil and gas industry over $1 billion (Jahanbakhshi, Keshavarzi, & Jahanbakhshi, 2012).

Wellbore instability is observed most often as sloughing and caving shale, resulting in hole enlargement, bridges and fill, tight hole in the formations which have time depend behaviors. The most common consequences are stuck pipe, sidetracks, logging and interpretation difficulties, and sidewall core recovery difficulties, difficulty running casing, poor cement jobs, and lost circulation. All contribute to increased costs, the possibility of losing part of the hole or the entire well, or reduced production (Jahanbakhshi et al., 2012).

Wellbore stability significantly contributes to non-productive time by incurring high amounts of drilling costs and increasing safety risks. Early detection of relevant wellbore stability issues is therefore crucial (Wessling, Bartetzko, Pei, & Dahl, 2012).

The most common well failure during drilling is borehole collapse. The method of analyzing this case involves the use of wellbore stability modeling consisting of a constitutive model coupled with a failure criterion. The constitutive model describes the deformation properties of the rock and the failure criterion determines the limits of the deformation (Lowrey & Ottesen, 1995).

As drilling advanced to deeper well depths, a controlled and managed drilling operation is required to minimize problems encountered during the process. Acquisition of drilling information

including downhole temperature and pressure is required to keep the drilling operation manageable and safe. Conventional Measurement-While-Drilling (MWD) system (Gravley, 1983) is the way to obtain these parameters in real time. However, MWD system has its limitations. Firstly, the MWD tool only measures the bottomhole variables since it is installed near the drill bit. Therefore, drilling parameters such as temperature and pressure over the entire wellbore cannot be accessed. Another limitation is that most MWD systems utilizing mud pulse telemetry have a low data transmission rate. Also, it requires money, manpower and time for operations and maintenance. This led to the development of an easy to operate, cost-effective, and accurate subsurface instrumentation system that measures distributed temperature and pressure over the entire drilled interval called Distributed Microchip System (DMS). (Yu et al., 2012)

1.2 PROBLEM STATEMENT

Due to large uncertainties of subsurface data such as rock Poisson ratio and permeability and impact of drilling fluid dynamics and density, the prediction of wellbore failure probability poses a challenge, the prediction can't be done through any simple correlation or observation. It is only possible by constructing a large database containing these attributes from many fields and analyzed through machine learning through extensive training on models.

1.3 OBJECTIVES OF THE RESEARCH

The objectives of this project are to study the influencing parameters controlling wellbore failure and how to predict the probability of its occurrence based on formation and mud knowledge. In order to achieve these objectives, the following scope of work have been conducted in this study:

- ✓ Literature survey for types/modes of wellbore failure during drilling a well.

- ✓ Identify existing models in literature that can quantify wellbore failure. Particularly on the temperature/pressure of drilling fluids in the wellbore.
- ✓ Probabilistic analysis of wellbore stability issues; particular on Bayesian algorithm for its prediction
- ✓ Based on cases field data, develop/test machine learning in identifying the probability of wellbore failure for given real-time pressure & temperature data.

1.4 OUTLAY OF THESIS

This chapter presents the background and motivation, as well as the objectives and scope of the research. Chapter 2 reviews related literature to the wellbore stability problem to highlight technical gaps between reality and practices. Chapter 3 outlines the major elements in the work flow which include data assembly, failure criterion determination and prediction using Gaussian Naïve Bayes algorithm before presenting the results in chapter 4. Chapter 5 summarizes the main findings of the research and gives some recommendations for future work.

CHAPTER 2

LITERATURE REVIEW AND THEORY

2.1 WELLBORE STABILITY

Wellbore stability is the term used in the oil and gas industry to describe the usable condition of the borehole during drilling operations. A usable hole must accommodate logging or any open hole evaluation, casing run and any other drilling activities trouble free. Wellbore instability occurs when there is either breakout or borehole collapse (Elijah, 2013). This is illustrated in Figure 2.1

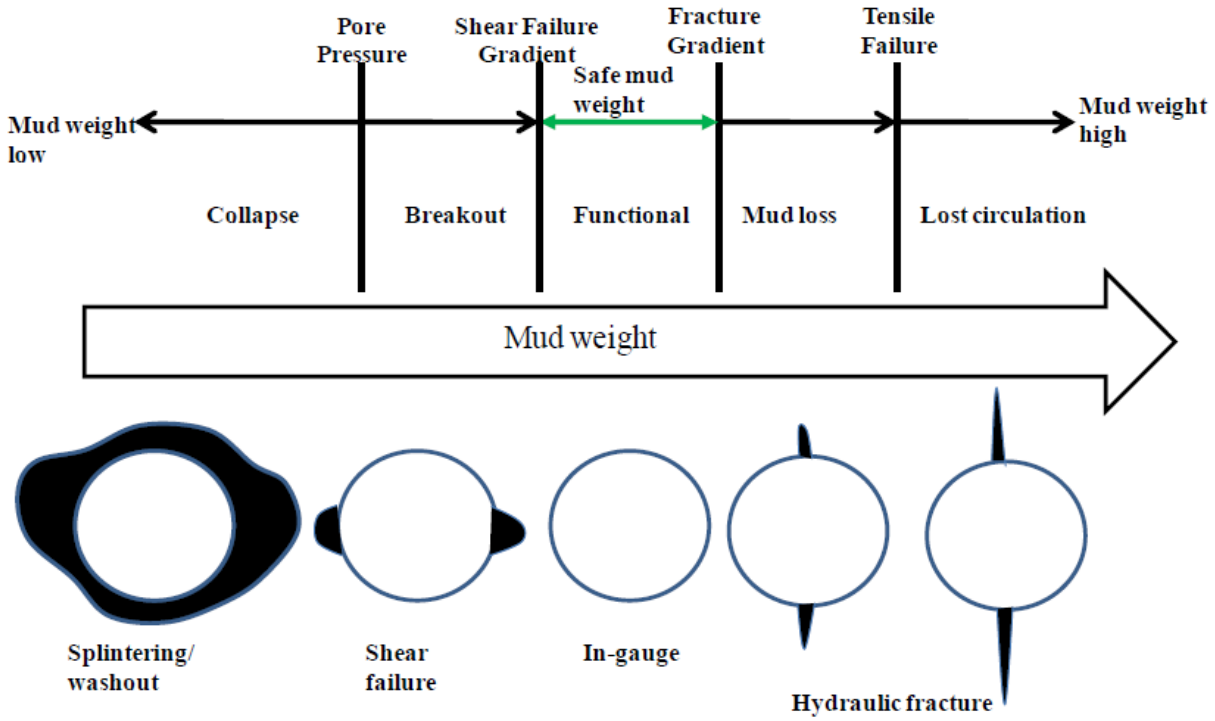

Figure 2. 1: **Schematic relationship of mud pressure (mud weight) and wellbore failure (Lang, Li, & Zhang, 2011)**

Wellbore instability (WI) is recognized when the hole diameter is markedly different from the bit size and the hole does not maintain its structural integrity (Osisanya, 2012).

According to Bernt Aadnoy, Cooper, Miska, Mitchell, and Payne (2009), wellbore instabilities include such phenomena as:

(i) breaking of intact rock around the wellbore due to high-stress concentration or sudden temperature variations,

(ii) loosening of rock fragments,

(iii) fracture extension from the wellbore into the formation, sometimes with a significant loss of drilling fluid.

WI also consists of mechanisms such as failure of rock around the borehole due to interaction with drilling fluid, squeezing of soft rocks such as salt and shales into the wellbore, and activation of pre-existing faults that intersect the wellbore.

2.2 MECHANISMS OF WELLBORE FAILURE

The two well-known mechanisms are shear (compressive) and tensile failures (BS Aadnoy & Chenevert, 1987; Bradley, 1979).

2.2.1 Shear Failure

The Von Mises Yield Condition and Mohr-Coulomb Shear Failure Criterion (BS Aadnoy & Chenevert, 1987) are the most commonly used hypotheses for evaluating rock shear failure. Von Mises considers the three principal in-situ stresses in wellbore compressive failures. These failure criteria are given as:

$$J_2{}^{1/2} = \sqrt{{}^{1}/_{6}\,[(\sigma_1 - \sigma_2)^2 + (\sigma_2 - \sigma_3)^2 + (\sigma_3 - \sigma_1)^2]} \qquad (2.1)$$

And

$$S - p_{fm} = {}^{1}/_{3}\,(\sigma_1 + \sigma_2 + \sigma_3) - p_{fm} \qquad (2.2)$$

The Mohr-Coulomb Model for shear failure neglects the intermediate principal stress (BS Aadnoy & Chenevert, 1987). This model predicts a minimum mud pressure that can cause wellbore collapse. For all well configurations, the maximum stress is the tangential stress, followed by the axial stress, and the radial stress (mud pressure).

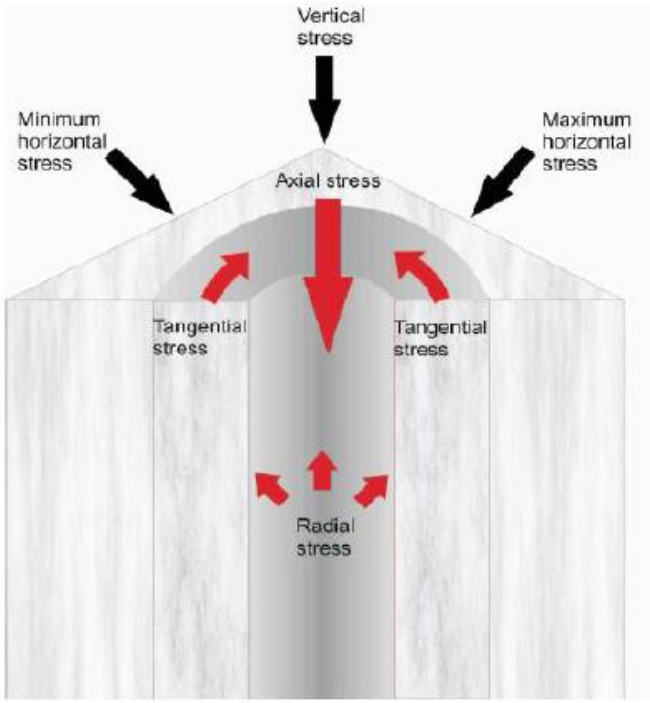

Figure 2. 2: **Stress distribution around a wellbore (Pašić, Gaurina Međimurec, & Matanović, 2007)**

Wellbore collapse is due to shear failure of rock around a borehole. To prevent this from occurring during drilling, mud pressure must be sufficiently high such that it will effectively support most of the load caused by the in situ stresses.

2.2.2 Tensile Failure

Generally, rocks are weak in tension. In most cases, the tensile strength of rock (σ_t) is set to zero (BS Aadnoy & Chenevert, 1987; Bradley, 1979), on the premise that drilling-induced fractures initiate in flaws, joints or pre-existing fractures around the wellbore.

The analysis of tensile failure involves the application of the effective stress concept (BS Aadnoy & Chenevert, 1987). This implies that a formation fails in tension when the least effective principal stress exceeds the rock tensile strength. An increase in the mud pressure will cause effective tangential stress to decrease. At a certain mud pressure, the value of the hoop stress becomes zero, and a vertical fracture initiates as the stress goes into tension. Thus, drilling-induced fractures are associated with minimum tangential stress (Bernt Aadnoy et al., 2009). By convention, the critical fracturing pressure is the mud pressure beyond which a wellbore will fracture in tension.

Considering the two wellbore failure mechanisms, too high a mud pressure will cause borehole fracturing, sometimes with a loss of drilling fluid into the formation. Not having sufficient well pressure capable of supporting load caused by high stress concentration around the wellbore can lead to a wellbore collapse. Here, it is assumed that the collapse pressure is higher than the pore pressure, so that well control is not the main issue.

At each formation interval, defining optimal mud pressure that will prevent collapse failure and maintain gauge hole without fracturing is the most challenging aspect of wellbore stability

analyses. Thus, a successful drilling operation requires a balance in mud weight and this is illustrated graphically in Figure 2.10 (Bradley 1979). The ability of drilling mud engineers to achieve successful mud programs mainly depends of the accuracies of collapse and fracture pressure prognoses prior to drilling operation (Udegbunam, Aadnøy, & Fjelde, 2014).

2.3 CAUSES OF WELLBORE INSTABILITY

Wellbore instability is usually caused by a combination of factors which may be broadly classified as being either controllable or uncontrollable (natural) in origin. These factors are shown in Table 2.1 (Bowes & Procter, 1997; Chen, Tan, & Haberfield, 2002; McLellan, 1996; Mohiuddin, Awal, Abdulraheem, & Khan, 2001).

Table 2. 1**: Causes of Wellbore Instability**

Causes of Wellbore Instability	
Uncontrollable (Natural) Factors	**Controllable Factors**
Naturally Fractured or Faulted Formations	Bottom Hole Pressure (Mud Density)
Tectonically Stressed Formations	Well Inclination and Azimuth
High In-situ Stresses	Transient Pore Pressures
Mobile Formations	Physical/chemical Rock-Fluid Interaction
Unconsolidated Formations	Drill String Vibrations
Naturally Over-Pressured Shale Collapse	Erosion
Induced Over-Pressured Shale Collapse	Temperature

2.4 UNCONTROLLABLE FACTORS

2.4.1 Naturally Fractured or Faulted Formations

2.4.1.1 Description

A natural fracture system in the rock can often be found near faults. Rock near faults can be broken into large or small pieces. If they are loose they can fall into the wellbore and jam the string in the hole. Even if the pieces are bonded together, impacts from the Bottom Hole Assembly (BHA) due to drill string vibration can cause the formation to fall into the wellbore. This type of sticking is particularly unusual in that stuck pipe can occur while drilling. The first sign of this problem is the string torquing up and sticking. There is a risk of sticking in fractured/faulted formation when drilling through a fault and when drilling through fractured limestone formations.

This mechanism can occur:

- in tectonically active zones.
- in prognosed fractured limestone.
- as the formation is drilled.

2.4.1.2 Preventative Action

To minimize drill string vibration, the operator can choose an alternative Rotation Per Minute (RPM) or change the BHA configuration if high shock vibrations are observed. The trip speed should be slowed before the BHA enters a suspected fractured/faulted area. Generally, the hole should be circulated clean before drilling ahead and the tripping speed should be restricted when BHA is opposite fractured formations and fault zones. To avoid pressure surges to the wellbore,

one should start/stop the drill string slowly and anticipate reaming during trips and ream fractured zones cautiously (Bowes & Procter, 1997).

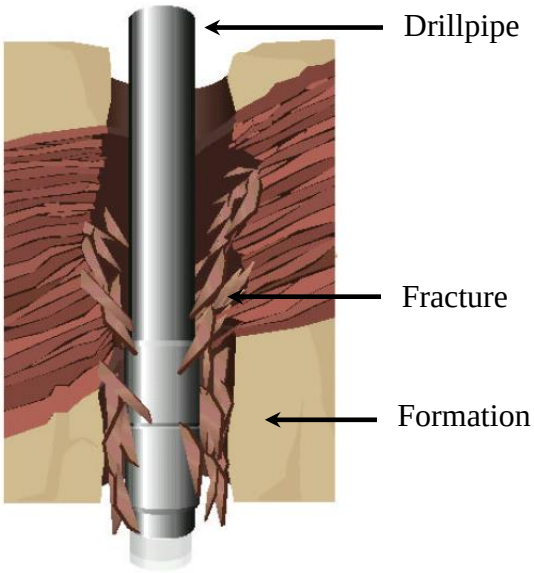

Figure 2. 3: **Naturally Fractured or Faulted Formation (Bowes & Procter, 1997)**

2.4.2 Tectonically Stressed Formations

2.4.2.1 Description

Wellbore instability is caused when highly stressed formations are drilled and there exists a significant difference between the near wellbore stress and the restraining pressure provided by the drilling fluid density.

Tectonic stresses build up in areas where rock is being compressed or stretched due to the movement of the earth's crust. The rock in these areas is being buckled by the pressure of moving tectonic plates.

When a hole is drilled in an area of high tectonic stresses, such as in or near mountainous regions, the rock around the wellbore will collapse into the wellbore and produce splintery cavings similar to those produced by over-pressured shale. In the tectonic stress case, the hydrostatic pressure required to stabilize the wellbore may be much higher than the fracture pressure of the other exposed formations.

2.4.2.2 Preventative Action

An operator should plan to case off these formations as quickly as possible and maintain mud weight within planned mud weight window. Wellbore instability shows itself as a hole cleaning problem. These formations should be drilled in smaller hole sizes to minimize the impact of a hole cleaning problem. It is also ensured that the circulation system is capable of handling the additional volume of cavings often associated with this mechanism (Bowes & Procter, 1997).

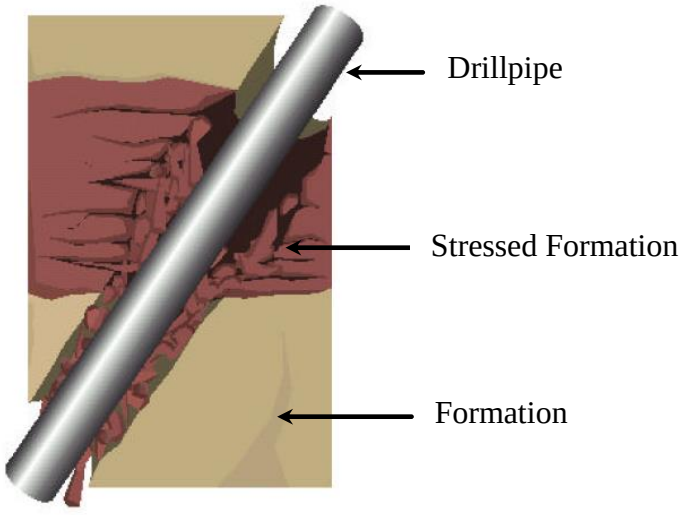

Figure 2. 4: **Tectonically Stressed Formation (Bowes & Procter, 1997).**

2.4.3 High In-Situ Stresses

2.4.3.1 Description

Anomalously height in-situ stresses, such as may be found in the vicinity of salt domes, near faults, or in the inner limbs of folds may give rise to wellbore instability (Pašić et al., 2007). Stress concentrations may also occur in particularly stiff rocks such as quartzose sandstones or conglomerates. Only a few case histories have been described in the literature for drilling problems caused by local stress concentrations, mainly because of the difficulty in measuring or estimating such in situ stresses (Pašić et al., 2007).

2.4.4 Mobile Formations

2.4.4.1 Description

The mobile formation such as salt formation squeezes into the wellbore because it is by the overburden forces during drilling process. Mobile formations behave in a plastic manner and deforming under pressure. The deformation results in a decrease in the wellbore size, causing problems running BHA's, logging tools and casing. A deformation occurs because the mud weight is not sufficient to prevent the formation from squeezing into the wellbore.

2.4.4.2 Preventative Action

The drilling operator should maintain sufficient mud weight and select an appropriate mud system that will not aggravate the mobile formation. A plan should be in place for frequent reaming/wiper trips particularly for this section of the hole and slow trip speed before BHA enters the suspected area. Minimize the open hole exposure time of these formations and Consider bi-centre Polycrstaline Diamond Compacts (PDC) bits. To allow a controlled washout with mobile salts, consider using a slightly under-saturated mud system (Bowes & Procter, 1997).

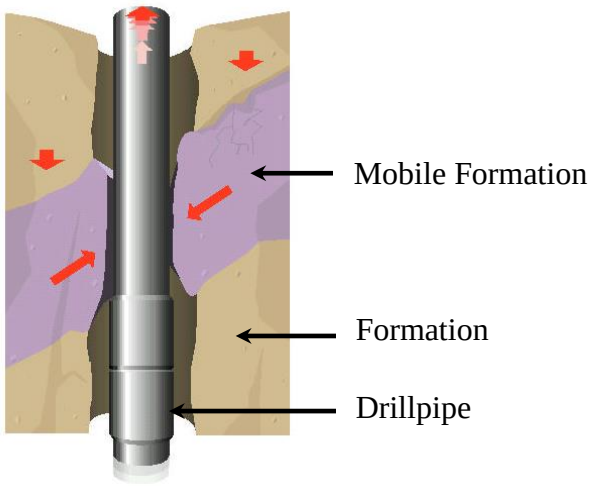

Figure 2. 5: **Mobile Formations (Bowes & Procter, 1997)**

2.4.5 Unconsolidated Formation

2.4.5.1 Description

An unconsolidated formation falls into the wellbore because it is loosely packed with little or no bonding between particles, pebbles or boulders. The collapse of the formation is caused by removing the supporting rock as the well is drilled. This is very similar to digging a hole in the sand on the beach, the faster you dig the faster the hole collapses. It happens in a wellbore when little or no filter cake is present. The un-bonded formation (sand, gravel, small river bed boulders, etc.) cannot be supported by hydrostatic overbalance as the fluid simply flows into the formation. Sand or gravel then falls into the hole and packs off the drill string. The effect can be a gradual increase in drag over a number of meters or can be sudden. This mechanism is normally associated with shallow formations. Examples are shallow river bed structures at about 500m in the central North Sea and in surface hole sections of land wells.

2.4.5.2 Preventative Action

These formations need an adequate filter cake to help stabilize the formation. Seepage loss can be minimized with fine lost circulation material. If possible, avoid excessive circulating time with the BHA opposite unconsolidated formations to reduce hydraulic erosion. Spot a gel pill before Pull out of the hole (POOH). Slow down tripping speed when the BHA is opposite unconsolidated formations to avoid mechanical damage.

Start and stop the pumps slowly to avoid pressure surges being applied to unconsolidated formations. Control-drill the suspected zone to allow time for the filter cake to build up, minimize annulus loading and resultant ECD's. Use sweeps to help keep the hole clean. Be prepared for shaker, desilter and desander overloading.

A method successfully used in the North Sea is to drill 10m, pull back to the top of the section and wait 10 minutes. Note any fill on the bottom when returning to drill ahead. If the fill is significant then ensure the process is repeated every 10m. It may be impossible to prevent the hole collapsing. If so let the hole stabilize itself with the BHA up out of harm's way (Bowes & Procter, 1997).

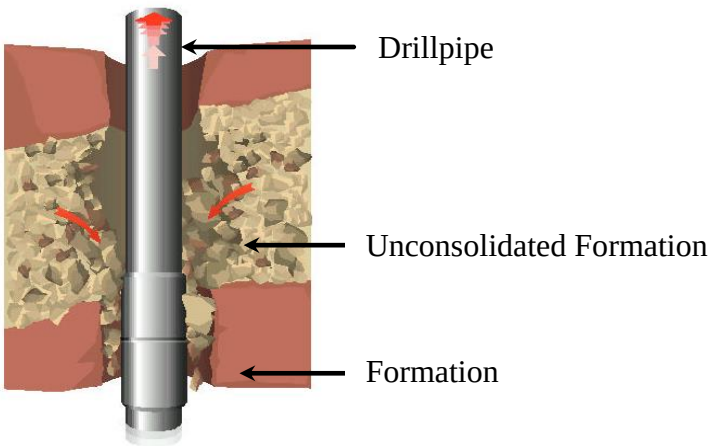

Figure 2. 6: **Unconsolidated Formation (Bowes & Procter, 1997).**

2.4.6 Naturally Over-Pressured Shale Collapse

2.4.6.1 Description

A naturally over-pressured shale is one with a natural pore pressure greater than the normal hydrostatic pressure gradient (0.433 psi/ft). Naturally over-pressured shales are most commonly caused by geological phenomena such as under-compaction, naturally removed overburden (i.e. weathering) and uplift. Using insufficient mud weight in these formations will cause the hole to become unstable and collapse.

2.4.6.2 Preventative Action

Plan to minimize hole exposure time and ensure planned mud weight is adequate. Rigorous use of gas levels to detect pore pressure trends and use of other information to predict pore pressure trends (for example Dexp). Once the shale has been exposed do not reduce the mud weight. It may also be the case that the mud weight will need to be raised with an increase in inclination (Bowes & Procter, 1997).

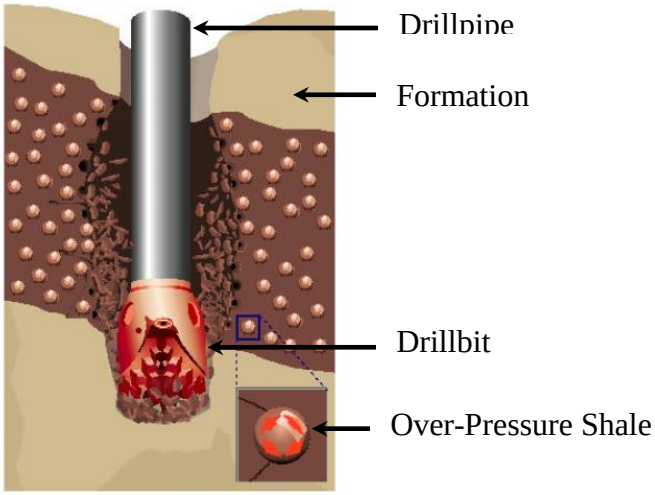

Figure 2. 7: **Naturally Over-Pressure Shale Collapse (Bowes & Procter, 1997)**

2.4.7 Induced Over-Pressure Shale Collapse

2.4.7.1 Description

Induced over-pressure shale occurs when the shale assumes the hydrostatic pressure of the wellbore fluids after a number of days of exposure to that pressure.

When this is followed by no increase or a reduction in hydrostatic pressure in the wellbore, the shale, which now has a higher internal pressure than the wellbore, collapses in a similar manner to naturally over-pressured shale.

This mechanism normally occurs:

- In Water Based Mud.
- After a reduction in mud weight or after a long exposure time during which the mud weight was constant.
- In the casing rat hole.

2.4.7.2 Preventative Action

Non water-based muds prevent inducing over-pressure in shale. Do not plan a reduction in mud weight after exposing shale. If cavings occur, utilize good hole cleaning practices (Bowes & Procter, 1997).

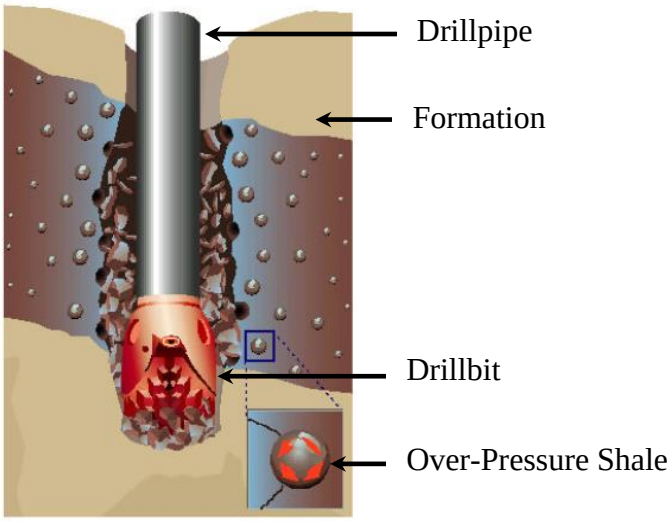

Figure 2. 8: **Induced Over-Pressure Shale Collapse (Bowes & Procter, 1997)**

2.5 CONTROLLABLE FACTORS

2.5.1 Bottom Hole Pressure (Mud Density)

Depending upon the application, either the bottom hole pressure, the mud density or the equivalent circulating density (ECD), is usually the most important determinant of whether an open wellbore is stable (Figures 2.9 and 2.10) (Gaurina-Međimurec, 1998; Hawkes & McLellan, 1999). The supporting pressure offered by the static or dynamic fluid pressure during either drilling, stimulating, working over or producing of a well, will determine the stress concentration present in the near wellbore vicinity.

Because rock failure is dependent on the effective stress the consequence for stability is highly dependent on whether and how rapidly fluid pressure penetrate the wellbore wall. That is not to say, however, that high mud densities or bottom hole pressures are always optimal for avoiding instability in a given well. In the absence of an efficient filter cake, such as in fractured formations,

a rise in a bottom hole pressure may be detrimental to stability and can compromise other criteria, e.g., formation damage, differential sticking risk, mud properties, or hydraulics (McLellan, 1996; Mohiuddin et al., 2001; Tan & Willoughby, 1993).

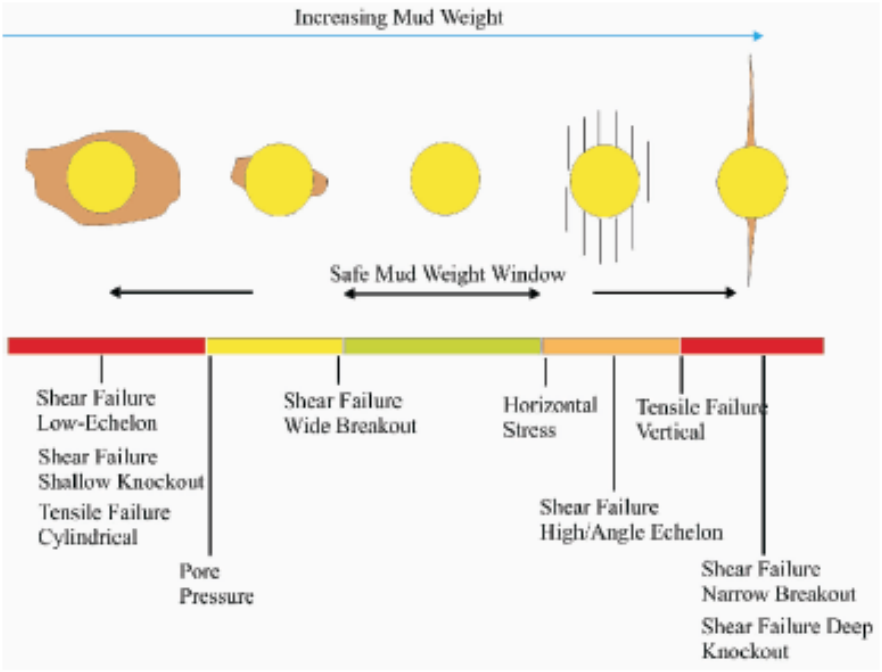

Figure 2. 9: **Effect of Mud Weight on the Stress in Wellbore Wall**

2.5.2 Well Inclination and Azimuth

Inclination and azimuthal orientation of a well with respect to the principal in-situ stresses can be an important factor affecting the risk of collapse and/or fracture breakdown occurring (Figure 2.8). This is particularly true for estimating the fracture breakdown pressure in tectonically stressed regions where there is strong stress anisotropy (McLellan, 1996).

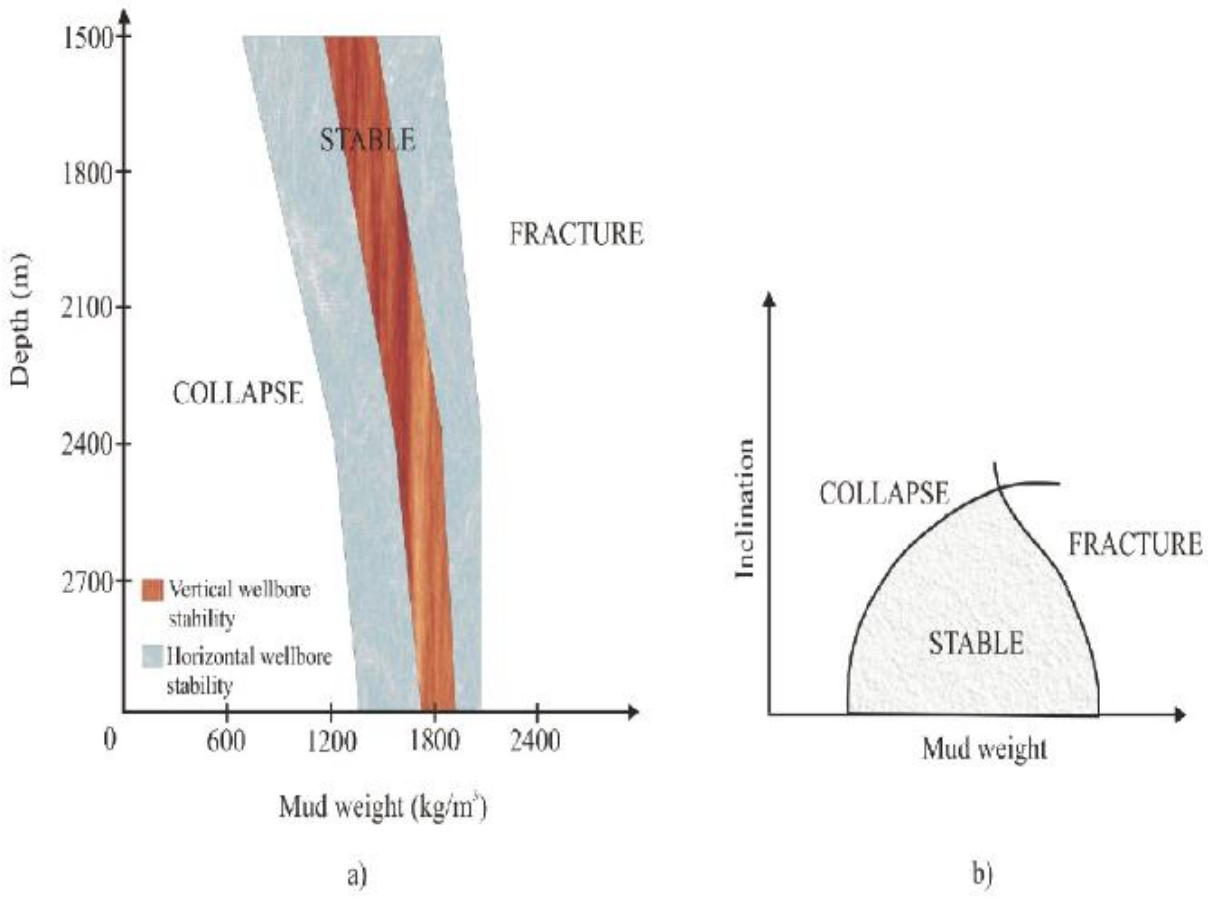

Figure 2. 10: **Effect of (a) The Well Depth and (b) Hole Inclination on Wellbore Stability**

2.5.3 Transient Wellbore Pressures

Transient wellbore pressures, such as swab and surge effects during drilling, may cause wellbore enlargement (Hawkes & McLellan, 1999). Tensile spalling can occur when the wellbore pressure across an interval is rapidly reduced by the swabbing action of the drill string for instance. If the formation has a sufficiently low tensile strength or is pre-fractured, the imbalance between the pore pressures in the rock and the wellbore can literally pull loose rock off the wall. Surge pressures can also cause rapid pore pressures increases in the near-wellbore area sometimes causing an immediate loss in rock strength which may ultimately lead to collapse. Other pore pressure

penetration-related phenomena may help to initially stabilize wellbores, e.g. filter cake efficiency in permeable formations, capillary threshold pressures for oil-based muds and transient pore pressure penetration effects (McLellan, 1996).

2.5.4 Physical/Chemical Fluid-Rock Interaction

There are many physical/chemical fluid-rock interaction phenomena which modify the near-wellbore rock strength or stress. These include hydration, osmotic pressures, swelling, rock softening and strength changes, and dispersion. The significance of these effects depend on a complex interaction of many factors including the nature of the formation (mineralogy, stiffness, strength, pore water composition, stress history, temperature), the presence of a filter cake or permeability barrier is present, the properties and chemical composition of the wellbore fluid, and the extent of any damage near the wellbore (McLellan, 1996).

2.5.5 Drillstring Vibrations (During Drilling)

Drillstring vibrations can enlarge holes in some circumstances. Optimal bottomhole assembly (BHA) design with respect to the hole geometry, inclination, and formations to be drilled can sometimes eliminate this potential contribution to wellbore collapse. Some authors claim that hole erosion may be caused due to a too high annular circulating velocity. This may be most significant in a yielded formation, a naturally fractured formation, or an unconsolidated or soft, dispersive sediment. The problem may be difficult to diagnose and fix in an inclined or horizontal well where high circulating rates are often desirable to ensure adequate hole cleaning (McLellan, 1996).

2.5.6 Drilling Fluid Temperature

Drilling fluid temperatures, and to some extent, bottomhole producing temperatures can give rise to thermal concentration or expansion stresses which may be detrimental to wellbore stability. The reduced mud temperature causes a reduction in the near-wellbore stress concentration, thus preventing the stresses in the rock from reaching their limiting strength (McLellan, 1996).

2.6 QUALITY ASSURANCE OF WELLBORE STABILITY ANALYSIS

D. A. Nguyen, Miska, Yu, and Saasen (2010) outlined some rules that should be followed to ensure the quality of wellbore fracture and wellbore collapse studies.

1. Prepare all data in the best possible way. In particular, identify parameters that are measured and those that are just assumed. You may also label assumed data as less precise.

2. After performing analysis investigate space to test if the results are within the expected range, for example by imposing stress bounds.

3. Calibrate model with measured fracture data, directions of wellbore breakout and possible fracture traces. Identify discrepancies between these. If there are inconsistencies either the data or the model is wrong. This should be clearly stated in the report.

4. Invoking the “reciprocity principle”. In using the model for prediction for other wells or other well sections, use exactly the same procedure and data basis as when developing the model.

5. Extrapolate the model to shallower and deeper depths and define the depth interval where it predicts reasonable results.

6. Assess the uncertainty in the model. If no calibration data exist the uncertainty may be large. Using the inversion model with many data reduces the uncertainty to a minimum.

2.7 ROCK FAILURE CRITERIA

In this section, a brief review of three failure criteria are presented. It should be noted that in the equations developed here for wellbore stability analysis, the pore pressure term was discarded since the stresses obtained through well log analysis will be effective stresses. Also, in this study we only consider vertical wellbores (Gholami, Moradzadeh, Rasouli, & Hanachi, 2014).

2.7.1 Mohr-Coulomb Criterion

Mohr-Coulomb shear failure criterion is mostly used in different engineering applications. In this criterion, shear failure takes place across a plane when the normal stress σ_n and the shear stress τ across this plane are associated with a functional relation characteristic of the material (Mohr, 1900):

$$\tau = c + \mu\sigma_n \tag{2.3}$$

where c is the cohesion and μ is the coefficient of internal friction of the material. The linearized form of the Mohr failure criterion may also be written in the principal stress space as

$$\sigma_1 = \sigma_c + N\sigma_3 \tag{2.4}$$

$$N = \left[(\mu^2 + 1)^{1/2} + \mu\right]^2 = tan^2\left(\frac{\pi}{4} + \frac{\varphi}{2}\right) \tag{2.5}$$

where σ_1 is the major principal effective stress at failure, σ_3 is the minimum principal effective stress at failure, σ_c is the uniaxial compressive strength (UCS), and φ is the angle of internal friction equivalent to arctan μ. As it was mentioned, this failure criterion assumes that the intermediate principal stress has no influence on failure and considers a linear model for obtaining the strength of the materials.

Table 2. 2: **Mohr-Coulomb criterion for determination of breakout pressure in vertical wellbores.**

$\boldsymbol{\sigma_1 \geq \sigma_2 \geq \sigma_3}$	Wellbore failure will occur if $\boldsymbol{P_w \leq P_{w(BO)}}$
$\boldsymbol{\sigma_z \geq \sigma_\theta \geq \sigma_r}$	$\boldsymbol{P_{w(BO)}} = (E - \sigma_c)/N$
$\boldsymbol{\sigma_\theta \geq \sigma_z \geq \sigma_r}$	$\boldsymbol{P_{w(BO)}} = (D - \sigma_c)/(1 + N)$
$\boldsymbol{\sigma_\theta \geq \sigma_r \geq \sigma_z}$	$\boldsymbol{P_{w(BO)}} = D - \sigma_c - NE$

Table 2. 3**: Mohr-Coulomb criterion for determination of fracture pressure in vertical wellbores.**

$\boldsymbol{\sigma_1 \geq \sigma_2 \geq \sigma_3}$	Wellbore fracture will occur if $\boldsymbol{P_w \geq P_{w(Frac)}}$
$\boldsymbol{\sigma_r \geq \sigma_\theta \geq \sigma_z}$	$\boldsymbol{P_{w(Frac)}} = \sigma_c + NB$
$\boldsymbol{\sigma_r \geq \sigma_z \geq \sigma_\theta}$	$\boldsymbol{P_{w(Frac)}} = (\sigma_c + NA)/(1 + N)$
$\boldsymbol{\sigma_z \geq \sigma_r \geq \sigma_\theta}$	$\boldsymbol{P_{w(Frac)}} = (\sigma_c - B)/N + A$

The mode of shear failure may be different depending on the order of magnitude of three principal stresses around the wellbore wall. These stresses are σ_θ, σ_r and σ_z. It has been found that the case of $\sigma_\theta \geq \sigma_z \geq \sigma_r$ is the most commonly encountered stress state corresponding to borehole breakout for all in situ stresses regimes. On the other hand, $\sigma_r \geq \sigma_z \geq \sigma_\theta$ is the most commonly stress regime corresponding to borehole fracture (Al-Ajmi & Zimmerman, 2005).

In the shear failure case, considering $\sigma_\theta = \sigma_1$, $\sigma_z = \sigma_2$ and $\sigma_r = \sigma_3$, substituting these values in the Mohr–Coulomb failure criterion presented in Eq. (2.4), the lower limit of the mud pressure in order to avoid breakouts, $P_{w(BO)}$, will be

$$\boldsymbol{P_{w(BO)}} = \frac{(D-\sigma_c)}{(1+N)} \qquad (2.6)$$

If the well pressure falls below $P_{w(BO)}$, borehole collapse will take place. Following the same procedure, the minimum allowable mud pressure to avoid breakouts around the wellbore wall corresponding to the other two possible orders of stress magnitudes can be calculated. The results of such calculations are presented in Table 2.2.

As discussed previously, borehole fracturing, corresponding to the tensile failure of formation, will occur if the well pressure rises above the fracture initiation pressure, $P_{w(Frac)}$. Thus, the upper bound for mud weight windows can be calculated. Considering the order of stress magnitudes around the wellbore, $P_{w(Frac)}$ was calculated and the results are summarized in Table 2.3.

It is well known that the Mohr-Coulomb criterion overestimates the tensile strength of rocks (Al-Ajmi & Zimmerman, 2005). Therefore, to use this criterion for tensile strength determination, a tensile cut-off should be considered. The tensile cut-off is defined as the minimum tangential stress around the wellbore wall (L. Zhang, Cao, & Radha, 2010):

$$\sigma_3 = T \tag{2.7}$$

Where T is the uniaxial tensile strength of rock. This equation implies that if a tensile failure occurs, the wellbore pressure, i.e. mud weight, should exceed the minimum tangential stress plus the tensile strength of the formation. In vertical wellbores, it is assumed that the tangential stress is the only tensile stress at the borehole wall. Introducing the equation for minimum tangential stress into Eq. (2.7), the upper limit of the mud pressure for the tensile cut-off is obtained as

$$P_{w(cut-off)} = 3\sigma_h - \sigma_H - T \tag{2.8}$$

The mud pressure estimated from this equation should be compared with the value obtained for $P_{w(Frac)}$ given from those presented in Table 2.3. The smaller one of these values should be considered as the maximum allowable mud pressure to avoid tensile induced fracture in the formation.

2.7.2 Hoek-Brown criterion

The Hoek–Brown empirical rock failure criterion (Hoek & Brown, 1980) was developed in the early 1980s for prediction of ultimate strength of intact rock and rock masses. Over the years, the Hoek–Brown rock mass failure criterion has undergone numerous revisions (Hoek and Brown, 1988, 1997; Hoek et al., 1992, 1995, 2002). It has even been adapted to specific rock masses (Hoek et al., 1998). A summary of the changes to the Hoek–Brown failure criterion throughout its development is given by Hoek and Marinos (2007). This empirical criterion uses the UCS of the intact rock material as a scaling parameter and introduces two dimensionless strength parameters, m and s. After studying a wide range of experimental data, Hoek and Brown (1980)stated that the relationship between the maximum and the minimum stresses at the point of failure is

$$\sigma_1 = \sigma_3 + \sigma_c \left(m \frac{\sigma_3}{\sigma_c} + 1 \right)^{1/2} \qquad (2.9)$$

where m and s are constants dependent on the properties of the rock. The Hoek–Brown failure criterion was originally developed for estimating the strength of rock masses for applications in excavation design, but it has then been developed and used for intact rocks too.

According to Hoek and Brown (1980, 1997), the parameter m depends on rock types. Table 2.4 gives the ranges of m-values for different rock types.

Table 2. 4**: Ranges of m-values recommended for different rock types.**

m-values	Rock types
$\mathbf{5 < m < 8}$	Carbonate rocks with well-developed crystal cleavage (e.g. dolomite, limestone, marble)
$\mathbf{4 < m < 10}$	Lithified argillaceous rocks (e.g. mudstone, siltstone, shale, slate)
$\mathbf{15 < m < 24}$	Arenaceous rocks with strong crystals and poorly developed crystal cleavage (e.g. sandstone, quartzite)
$\mathbf{16 < m < 19}$	Fine-grained polyminerallic igneous crystalline rocks (e.g. andesite, dolerite, diabase, rhyolite)
$\mathbf{22 < m < 33}$	Coarse-grained polyminerallic igneous and metamorphic rocks (e.g. amphibolite, gabbro, gneiss, granite, norite, quartz-diorite)

In underground space applications, Hoek–Brown failure criterion has widely been accepted as a better criterion compared to Mohr-Coulomb criterion since it fits a non-linear model to the data, as well as provides a better estimation of rock strength.

Similar calculation procedures described in the previous sub-section can be used to calculate mud pressures, corresponding to the lower and upper, stable mud weight windows by assuming the Hoek–Brown failure criterion. Tables 2.5 and 2.6 summarize the results. In equations presented in these tables, p and q depend on the UCS (σ_c) of rocks and can be obtained using the following equations:

$$p = m\sigma_c \tag{2.10}$$

$$q = {\sigma_c}^2 \tag{2.11}$$

Table 2. 5**: Hoek–Brown criterion for determination of breakout pressure in vertical wellbores.**

$\boldsymbol{\sigma_1 \geq \sigma_2 \geq \sigma_3}$	Wellbore failure will occur if $\boldsymbol{P_w \leq P_{w(BO)}}$
$\boldsymbol{\sigma_z \geq \sigma_\theta \geq \sigma_r}$	$\boldsymbol{P_{w(BO)}} = \dfrac{(2D+p) - \sqrt{(2E+p)^2 - 4E^2 + q}}{2}$
$\boldsymbol{\sigma_\theta \geq \sigma_z \geq \sigma_r}$	$\boldsymbol{P_{w(BO)}} = \dfrac{(4D+p) - \sqrt{(4D+p)^2 + 16q - 16D^2}}{8}$
$\boldsymbol{\sigma_\theta \geq \sigma_r \geq \sigma_z}$	$\boldsymbol{P_{w(BO)}} = \dfrac{2(D-E) - \sqrt{4(D-E)^2 - 4(D-E-pE-q}}{2}$

Table 2. 6**: Hoek–Brown criterion for determination of fracture pressure in vertical wellbores.**

$\boldsymbol{\sigma_1 \geq \sigma_2 \geq \sigma_3}$	Wellbore fracture will occur if $\boldsymbol{P_w \geq P_{w(Frac)}}$
$\boldsymbol{\sigma_r \geq \sigma_\theta \geq \sigma_z}$	$\boldsymbol{P_{w(Frac)}} = \dfrac{2B + \sqrt{4B^2 - 4(B^2 - pB + q)}}{2}$
$\boldsymbol{\sigma_r \geq \sigma_z \geq \sigma_\theta}$	$\boldsymbol{P_{w(Frac)}} = \dfrac{(4A-p) + \sqrt{(4A-p)^2 - 16(A^2 - pA - q)}}{8}$
$\boldsymbol{\sigma_z \geq \sigma_r \geq \sigma_\theta}$	$\boldsymbol{P_{w(Frac)}} = \dfrac{2(A-B) + \sqrt{[2(B-A)+p]^2 - 4[(B-A)^2 - pA + q]}}{2}$

2.7.3 Mogi-Coulomb criterion

In polyaxial stress states, Mogi (1971) indicated that brittle fracture always occurs along a plane striking in the intermediate principal stress direction. He suggested a new failure criterion as below:

$$\tau_{oct} = f(\sigma_{m,2}) \quad (2.12)$$

where f is a nonlinear, power-law function; $\sigma_{m,2}$ and τ_{oct} are respectively, the effective mean stress and the octahedral shearstress defined by

$$\sigma_{m,2} = \frac{\sigma_1+\sigma_3}{2} \quad (2.13)$$

$$\tau_{oct} = \frac{1}{3}\sqrt{(\sigma_1-\sigma_2)^2+(\sigma_2-\sigma_3)^2+(\sigma_3-\sigma_1)^2} \quad (2.14)$$

Parameters of this failure function cannot be easily related to the Coulomb strength parameters, c and φ (Colmenares & Zoback, 2002). Thus, Al-Ajmi and Zimmerman (2005) proposed that the function f can be considered to be a linear function as follows:

$$\tau_{oct} = a + b\sigma_{m,2} \quad (2.15)$$

Where

$$a = \frac{2\sqrt{2}}{3} c\, cos\varphi \quad (2.16)$$

$$b = \frac{2\sqrt{2}}{3} c\, sin\varphi \quad (2.17)$$

Eq. (2.15) is an extension of the linear Coulomb criterion into the Mogi stress domain referred to as Mogi–Coulomb failure criterion. The strengthening effect of the intermediate principal stress can be considered by applying the Mogi–Coulomb law. The first and second stress invariants, $I_1$and I_2, are defined by

$$I_1 = \sigma_1 + \sigma_2 + \sigma_3 \quad (2.18)$$

$$I_2 = \sigma_1\sigma_2 + \sigma_2\sigma_3 + \sigma_3\sigma_1 \quad (2.19)$$

Using the Mogi–Coulomb criterion, we will have

$$\sqrt{{I_1}^2 - 3{I_2}^2} = a' + b'(I_1 - \sigma_2) \quad (2.20)$$

Where

$$a' = 2c\ cos\varphi \quad (2.21)$$

$$b' = sin\varphi \quad (2.22)$$

The principal stresses at the borehole wall for shear failure to occur represent the highest stress concentration that may result in compressive failure. Introducing these equations into Eqs. (2.18) and (2.19), the first and second stress invariants will be changed to

$$I_1 = D + E \quad (2.23)$$

$$I_2 = DE + DP_w - {P_w}^2 \quad (2.24)$$

To determine the mud pressures corresponding to the lower and upper bounds of mud weight windows, we follow similar calculation procedures used in the two previous subsections, here, considering the Mogi–Coulomb criterion. The results are presented in Tables 2.7 and 2.8.

It is noted that the uniaxial tensile strength estimated by Mogi–Coulomb criterion is identical to that of Mohr-Coulomb criterion since both criteria are equivalent in the state of uniaxial tension. Therefore, a tensile cut-off should also be introduced into the Mogi–Coulomb failure criterion. Thus, the upper limit of the mud pressure defined by Eq. (2.8) should be introduced into the Mogi–Coulomb borehole failure criterion (Gholami et al., 2014).

Table 2. 7**: Mogi–Coulomb criterion for determination of breakout pressure in vertical wellbores.**

$\boldsymbol{\sigma_1 \geq \sigma_2 \geq \sigma_3}$	Wellbore failure will occur if $\boldsymbol{P_w \leq P_{w(BO)}}$
$\boldsymbol{\sigma_z \geq \sigma_\theta \geq \sigma_r}$	$\boldsymbol{P_{w(BO)}} = \frac{1}{6-2b'^2}\left[(3D+2b'K)+\sqrt{H+12(K^2+b'DK)}\right]$
$\boldsymbol{\sigma_\theta \geq \sigma_z \geq \sigma_r}$	$\boldsymbol{P_{w(BO)}} = \frac{1}{2}D-\frac{1}{6}\sqrt{12(a'+b'D)^2-3(D-2E)^2}$
$\boldsymbol{\sigma_\theta \geq \sigma_r \geq \sigma_z}$	$\boldsymbol{P_{w(BO)}} = \frac{1}{6-2b'^2}\left[(3D-2b'G)+\sqrt{H+12(G^2-b'DG)}\right]$

$$\boldsymbol{H = D^2(4b'^2-3)+(E^2-DE)(4b'^2-12), K = a'+b'E, G = K+b'D}$$

Table 2. 8**: Mogi–Coulomb criterion for determination of fracture pressure in vertical wellbores.**

$\boldsymbol{\sigma_1 \geq \sigma_2 \geq \sigma_3}$	Wellbore fracture will occur if $\boldsymbol{P_w \geq P_{w(Frac)}}$
$\boldsymbol{\sigma_r \geq \sigma_\theta \geq \sigma_z}$	$\boldsymbol{P_{w(Frac)}} = \frac{1}{6-2b'^2}\left[(3A+2b'N)+\sqrt{J+12(N^2+b'AN)}\right]$
$\boldsymbol{\sigma_r \geq \sigma_z \geq \sigma_\theta}$	$\boldsymbol{P_{w(Frac)}} = \frac{1}{2}A+\frac{1}{6}\sqrt{12(a'+b'A)^2-3(2AB)^2}$
$\boldsymbol{\sigma_z \geq \sigma_r \geq \sigma_\theta}$	$\boldsymbol{P_{w(Frac)}} = \frac{1}{6-2b'^2}\left[(3A+2b'M)+\sqrt{J+12(M^2-b'AM)}\right]$

$$\boldsymbol{J = D^2(4b'^2-3)+(E^2-DE)(4b'^2-12)\,, M = N+b'D, N = a'+b'(E-2P_0)}$$

2.8 WELLBORE TEMPERATURE MODEL

D. A. Nguyen et al. (2010) proposed a new wellbore stability model that incorporates thermal effects to account for drag forces created from the contacts between drillpipe and casing/formation during drilling and tripping formations. In summary, the wellbore temperature model is constructed based on balance of energy in a control volume. And finally, the wellbore stability model uses the traditional single point failure approach with consideration of hydraulic and thermally induced stresses. The complete schematic of the model is shown in Figure 2.11.

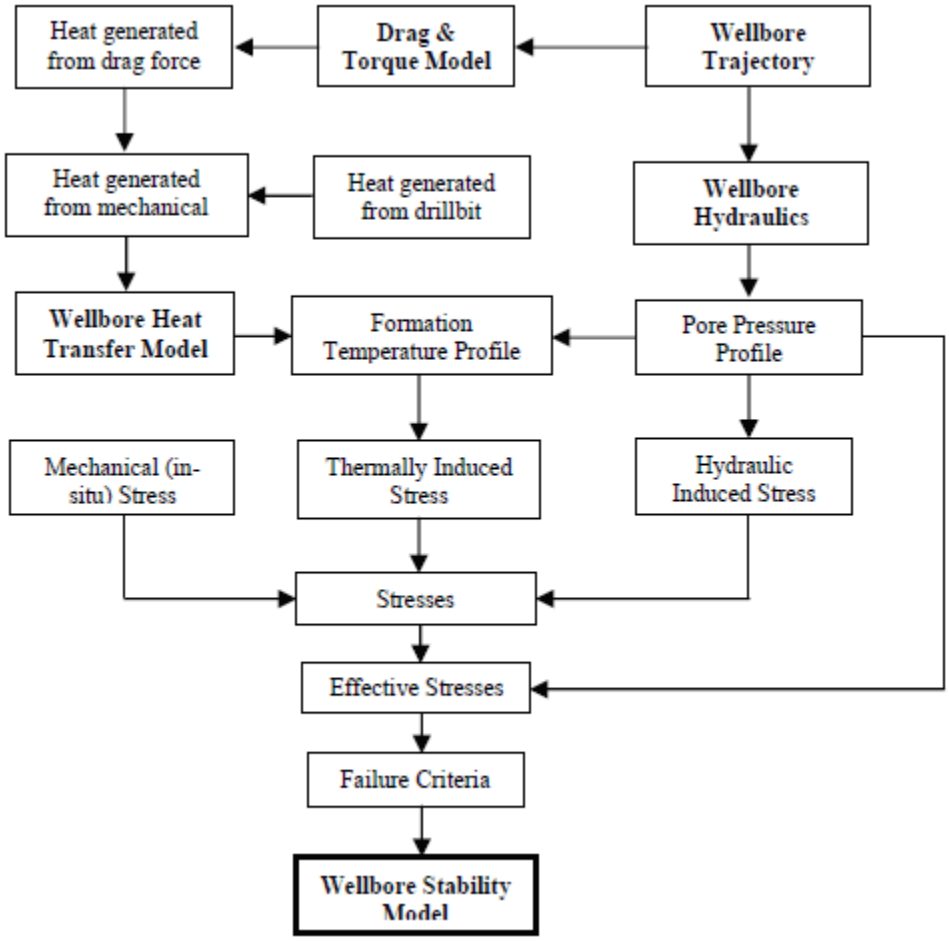

Figure 2. 11: **Model Algorithm** (D. A. Nguyen et al., 2010)

2.8.1 Wellbore Heat Transfer

Basic assumptions for the transient heat transfer model:

• Drilling fluid is incompressible with constant properties;

• Radiation heat transfer is negligible;

• Formation properties are independent of temperature;

• Radial temperature gradient of drilling fluid is negligible.

2.8.2 Thermo-Poro-Elastic Method

The thermo-poro-elastic model is obtained by superposing in-situ mechanical, hydraulic and thermal induced stress effects. The stress components (Fig. 2.12) can be expressed as follows:

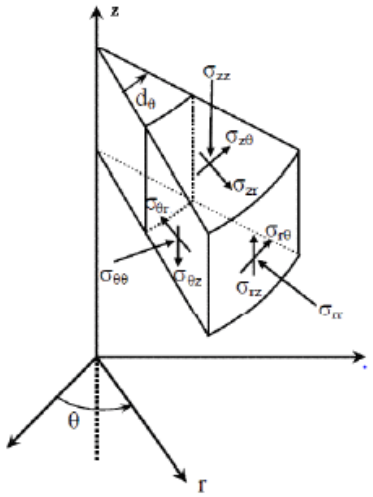

Figure 2. 12: **Stress Components in Cylindrical Coordinate System (D. A. Nguyen et al., 2010).**

$$\sigma_{rr} = \left(\frac{\sigma^o{}_{xx}+\sigma^o{}_{yy}}{2}\right)\left(1-\frac{r_w{}^2}{r^2}\right) + \left(\frac{\sigma^o{}_{xx}-\sigma^o{}_{yy}}{2}\right)\left(1+3\frac{r_w{}^4}{r^4}-4\frac{r_w{}^2}{r^2}\right)cos2\theta + \sigma^o{}_{xy}\left(1+3\frac{r_w{}^4}{r^4}-4\frac{r_w{}^2}{r^2}\right)sin2\theta + P_w\frac{r_w{}^2}{r^2} + \frac{\alpha_P(1-2v)}{1-v}\frac{1}{r^2}\int_{r_w}^{r}\Delta P(r',t)r'dr' - \frac{\alpha_T E}{1-v}\frac{1}{r^2}\int_{r_w}^{r}\Delta T_f(r',t)r'dr' - \alpha_T E\Delta T_w(t)\frac{r_w{}^2}{r^2}$$

$$\sigma_{\theta\theta} = \left(\frac{\sigma^o{}_{xx}+\sigma^o{}_{yy}}{2}\right)\left(1+\frac{r_w{}^2}{r^2}\right) - \left(\frac{\sigma^o{}_{xx}-\sigma^o{}_{yy}}{2}\right)\left(1+3\frac{r_w{}^4}{r^4}\right)cos2\theta - \sigma^o{}_{xy}\left(1+3\frac{r_w{}^4}{r^4}\right)sin2\theta - P_w\frac{r_w{}^2}{r^2} - \frac{\alpha_P(1-2v)}{1-v}\left[\frac{1}{r^2}\int_{r_w}^{r}\Delta P(r',t)r'dr' - \Delta P(r,t)\right] + \frac{\alpha_T E}{1-v}\left[\frac{1}{r^2}\int_{r_w}^{r}\Delta T_f(r',t)r'dr' - \Delta T_f(r,t)\right] + \alpha_T E\Delta T_w(t)\frac{r_w{}^2}{r^2}$$

$$\sigma_{zz} = \sigma^o{}_{zz} - v\left[2\left(\sigma^o{}_{xx}-\sigma^o{}_{yy}\right)\frac{r_w{}^2}{r^2}cos2\theta + 4\sigma^o{}_{xy}\frac{r_w{}^2}{r^2}sin2\theta\right] + \frac{\alpha_P(1-2v)}{1-v}\Delta P(r,t) - \frac{\alpha_T E}{1-v}\Delta T_f(r,t)$$

$$\sigma_{r\theta} = \sigma_{\theta r} = \left(\frac{\sigma^o{}_{yy}-\sigma^o{}_{xx}}{2}\right)\left(1-3\frac{r_w{}^4}{r^4}+2\frac{r_w{}^2}{r^2}\right)sin2\theta + \sigma^o{}_{xy}\left(1-3\frac{r_w{}^4}{r^4}+2\frac{r_w{}^2}{r^2}\right)cos2\theta$$

$$\sigma_{\theta z} = \sigma_{z\theta} = \left(-\sigma^o{}_{xz}sin\theta + \sigma^o{}_{yz}cos\theta\right)\left(1+\frac{r_w{}^2}{r^2}\right)$$

$$\sigma_{zr} = \sigma_{rz} = \left(\sigma^o{}_{xz}cos\theta + \sigma^o{}_{yz}sin\theta\right)\left(1-\frac{r_w{}^2}{r^2}\right) \qquad (2.25)$$

2.9 PRIOR WORK ON WELLBORE STABILITY MODELLING

Over time, quite a number of contributions have been made towards the maintenance of wellbore stability and integrity in various drilling and production scenarios, with more recent works being concentrated on the prediction of wellbore failure. A borehole stability analysis was carried out by Fuh, Deom, and Turner (1991). Before the drilling of the first horizontal well drilled in Block K/18 of the Dutch Sector of the North Sea Field, data from previous eight vertical wells drilled in the area were analyzed and used to construct a geomechanical model that simulated the potential behavior of the horizontal well under design. The challenge was to drill a high-angle hole through the highly reactive and potentially over-pressured Vlieland Shale, then into the partially depleted underlying Vlieland Sandstone. Borehole stability analysis provided useful information for the drilling of the horizontal well with few manageable problems of instability.

In 1992, (Santarelli, Dahen, Baroudi, & Sliman) presented a case study of drilling in highly fractured volcanic rocks at great depths. It was found that the main mechanism of instability was mud penetration in fractures that led to the eventual erosion of the wellbore wall due to inadequate wall support. By simulating the fractured rock mass using discrete element modeling (DEM), an appropriate mud weight was obtained. The use of this new mud weight proved successful.

Ong and Roegiers (1993) presented an anisotropic model for calculating the stress around the wellbore. They concluded that the borehole collapse is a manifestation of shear failure, which in a horizontal wellbore, is significantly affected by high degrees of rock anisotropy, high in-situ stress anisotropy, and excessive cooling of the wellbore. According to Ong S. H. et al, pore pressure and porous elastic constant also affect the shear failure but the effect is less pronounced.

Wong, Veeken, and Kenter (1994) proposed thick-walled-cylinder strength tests (TWC) that involved taking cores. Their method was used in deriving the necessary mechanical data used in borehole stability analysis for drilling a horizontal well in the North Sea. Based on their study, the elastic/brittle model prediction was shown to be unrealistically conservative. Nevertheless, the model qualitatively indicates the solution's sensitivity to different field input parameters. According to the authors, the TWC empirical approach is a new, simple method that provides a quick, qualitative borehole stability assessment. The elastoplastic analysis gives a realistic mud weight prediction, but it is the most expensive test to perform.

In 1991, lost time due to stuck pipe related drilling problems accounted for approximately 18% of total drilling time in Mobil Producing Nigeria (MPN) offshore operations. The primary cause of stuck pipe was identified as mechanical wellbore instability. In order to solve this problem, Lowrey and Ottesen (1995) reported that MPN has to carry out borehole stability study and the result was productive. Data acquisition involved taking conventional cores in the zone of interest, which can make the cost of borehole stability study unattractive. The parameters obtained were used to perform a geometrical simulation and estimate safe mud weights. Use of these mud weights led to a marked improvement in wellbore stability.

Sanchez D, Cabrera S, and Coll (1996) used borehole stability 2-D model to analyze the borehole condition under open hole completion in Venezuela. A 2-D finite element model was developed with a generalized plasticity constitutive equation. A safe drawdown to prevent failure was determined and the well was completed under an open hole without any production liner. The well produced above the estimated potential without any sanding or stability problems.

Fung, Wan, Rodriguez, and Bellorin (1996) also developed a finite element elastoplastic model that can perform effective stress analysis of the near wellbore tensile and shear failure. Their model is capable of handling extremely low confining stresses in unconsolidated formation. As plastic yielding occurs at relatively low deviatoric confining stress condition, it is not a good indication of wellbore failure in terms of loss of service. They, therefore, developed a more realistic criterion based on the accumulated plastic strain. The model was successfully used to analyze the stability of two horizontal wells with open-hole completion in unconsolidated oil sand.

Santarelli, Zaho, Burrafato, Zausa, and Giacca (1996) presented wellbore instability problems occurring in a developed field in Italy. The problems were analyzed with respect to the mud weights, mud types, stress regime, and azimuths. Based on the data obtained, drilling operations were successfully carried out with necessary modifications.

Cui, Abousleiman, Ekbote, Roegiers, and Zaman (1999) developed a software PBORE-3D for windows which is capable of performing stability analyses of boreholes. The model considers the fully coupled effects between the rock matrix and the pore fluid using recently-developed poroelastic borehole models. PBORE-3D was used to analyze stress/pore pressure, formation failure, and mud weight design.

For modeling naturally fractured reservoirs, J. Zhang and Roegiers (2000), developed a dual porosity poroelastic model that is effective and accurate in the characterization of stresses and flow fields. They also developed a generalized plane strain and dual porosity finite element solution for analyzing horizontal borehole stability. Their results show that horizontal borehole stability

depends strongly on the in-situ stress state, the borehole orientation, time, drilling fluid pressure and fracture characteristics.

Severe instability was encountered while some drilling horizontal drains in Hamlah-Gulailah formation, ABK field, offshore Abu Dhabi. In analyzing the instability problem, Onaisi, Locane, and Razimbaud (2000) reported that a comprehensive rock mechanical study was carried out to characterize the rock strength and in-situ horizontal stresses. The study suggested that the horizontal stresses were anisotropic in nature with strike-slip-thrust stress regimes. The rock mechanical simulation predicted higher mud weights than those actually used in the field.

de Fontoura, Holzberg, Teixeira, and Frydman (2002) presented three analytical methods for evaluating the influence of parameter uncertainties in the wellbore failure process: FOSM (First Order Second Moment), FORM (First Order Reliability Model) and SEAM (Statistical Error Analysis Method). They also presented the results of a sensitivity study to establish the most important parameters that control wellbore instability. This is necessary in order to limit the number of calculations before establishing the probability of failure. The results demonstrate the importance of reducing uncertainties associated with the relevant parameters by means of careful testing procedures. In general, the analyses indicated that in situ stresses and the formation pore pressure are always very important in wellbore stability analyses.

Morita (2004) presented a study on “Well Orientation Effect on Borehole Stability”. It was concluded that actual rocks are not linear elastic materials. Before a borehole collapse, the non-linearity of the rock deformation becomes significant. The significant non-linearity reduces the stress concentrations induced by directional in-situ loads. In addition, an oriented borehole has a

non-uniform stress or stress gradient around a borehole. The stress gradient reduces the stress concentration area. Since the smaller size of the stress concentrated region is less liable to fail then the wellbore stability is mostly controlled by the maximum radial stress after local failures, rather than the ratio of the radial principal stresses.

Simangunsong, Villatoro, and Davis (2006) reported that depending on the source of the problem, wellbore instability is classified either as mechanical or chemical. Chemical wellbore instability, often called shale instability, is most commonly associated with water adsorption in shaly formations, where the water phase is present and can cause borehole collapse. In contrast, mechanical wellbore instability is caused by applying mud of insufficient weight, which will create higher hoop stresses around the hole-wall. Hoop stresses around the hole-wall are often excessively high and result in rock failure. The most rapid remedy for this instability is to increase mud weight and/or adjust the well trajectory for high-angle wells. The mechanical instability occurs as soon as the new formation is drilled, but chemical instability is time dependent because shales are subject to strength alteration once exposed to different drilling fluids. A series of experimental studies led to the conclusion that shale strength decreases with time when the shale is exposed to most drilling fluids. Despite the tendency of shale to experience chemical instability, it can also experience mechanical instability simultaneously, which can lead to a more complex problem.

Mody, Tare, and Wang (2007) presented the need for sustainable deployment of geomechanics technology to reducing well construction costs. The major hurdles in borehole stability studies currently are often due to, but not limited to, the following factors:

1. The majority of easily accessible oil and gas reservoirs have already been exploited. The trend in hydrocarbon exploration is steadily moving to deeper and more complex environments (e. g., in deep water, sub-salt high-pressure high temperature (HPHT) and other challenging environments);

2. Data regarding rock mechanical properties, in-situ stress states, and geological structures cannot be accurately defined and are often provided with large uncertainties;

3. Well engineers, petro physicists and drillers who are directly involved in well delivery may not have adequate time and training in identifying and managing borehole instability issues;

4. Due to lack of resources and time constraints, well operations after action reviews typically get lower priority and as a consequence, these reviews may not be well documented.

Mody et al. (2007) also stated that borehole stability related downtime associated with well construction is typically 10-15 % of the total well cost and about 50 % of total non-productive time.

Drilling horizontal wells, single and multilateral, is a common practice for Saudi Aramco. For effective drilling and reservoir management, a borehole stability study was carried out by Bin Rabaa, Abass, Hembling, and Finkbeiner (2007). This was used to identify the optimum mud weight and well azimuth to place long-reach horizontal wells, so as to minimize the risk of stress-induced borehole breakouts. Also, to optimize drilling mud weights and to aid in making informed decisions about adequate completions designs, as well as ensure sustainable production under depletion modes. They concluded that under undepleted conditions, horizontal wells should be drilled with oil-based mud, parallel to the field-derived maximum principal horizontal stress

azimuth, in order to maximize borehole stability and minimize required mud weights during drilling and completion.

Pašić et al. (2007) presented causes, indicators and diagnosing of wellbore instability as well as the wellbore stresses model. They concluded that every well should be evaluated individually based on next criteria: the type of anticipated problems, their potential severity, the quantity and quality of data needed for a proper analysis, time and budget, and the success of previous analyses of particular type.

Sinha et al. (2008) presented an algorithm on how to estimate the rock stresses from borehole sonic data. Their work was only for sand reservoirs. However, borehole stability problems occur in shale.

V. X. Nguyen and Abousleiman (2009) developed an analytical poro-chemo-thermo-elastic solution for an inclined wellbore that coupled transient chemical and thermal effects on shale stability. The shale was modeled as an imperfect semi-permeable membrane which allows partial transport of solutes. In addition to chemical osmosis, both solute transport and thermal effects were taken into account to realistically model field conditions.

Tran and Abousleiman (2010) highlighted and prioritized various rock mechanical parameters, in-situ stresses and pore pressure conditions that affect wellbore instability with failure criteria frequently used in such analysis such as the Mohr-Coulomb, Drucker-Prager, modified Lade, and tensile failure. In addition, different far-field stress regimes including the normal fault, thrust fault, and strike-slip fault were considered in this study to evaluate the influence of such geological settings on parameter sensitivity for each of the failure criterion. The results showed that the

magnitude of impact of the various parameters depends on both the failure criterion in use and the regional far-field stress state.

Ottesen (2010) presented results from a geomechanical investigation of a wellbore instability incident experienced in a fractured shale formation. As part of this assessment, a preserved core was obtained from the fractured shale interval and the presence of fractures was identified both by CAT scan and visual inspection. A series of triaxial tests were conducted to characterize the mechanical properties and failure strength of this shale. This data, combined with wellbore stability modeling, suggests that the residual strength, rather than the peak failure strength, is a more representative measure of a fractured rock's in-situ strength.

D. A. Nguyen et al. (2010) conducted a study to examine the effect of temperature on the stability of the near wellbore region, taking into account the heat transfer between formation and flowing drilling fluid with the consideration of mechanical friction and associated heat sources. They proposed a new model that is applicable to directional and horizontal wells. The model incorporates thermal effects due to the drag forces created from the contacts between drillpipe and casing/formation during drilling and tripping operations. It is then utilized in a number of configurations of directional wells to study temperature profiles behaviors and their effects on wellbore stability. It is observed that the drilling fluid temperature is noticeably under-predicted by existing literature, and in some cases it can easily exceed the geothermal formation temperature if mechanical friction is taken into account. The formation temperature profile near the borehole region is also found to be considerably affected when wellbore heat transfer is considered, as opposed to the constant wall temperature approach in existing literature. These differences

alternate the temperature induced stresses and consequently change the mud weight window for wellbore stability prediction.

Soreide, Bostrom, and Horsrud (2009) studied the effect of anisotropy on shale borehole stability in high pressure and high temperature well. They concluded that the effect of anisotropy is most pronounced when drilling at high inclination angles, almost parallel to the bedding. A mixture of failure modes may also be observed.

Li and Purdy (2010) in their study on how to estimate maximum horizontal stress proposed two methods. The first method is based on a generalized Hooke's law, with coupling the equilibrium of three in-situ stress components and pore pressure. They believed that this new technique can reduce the uncertainty of in-situ stress prediction by narrowing the area of the conventional polygon of the in-situ stresses. The second method involves the analysis of drilling-induced near-wellbore stresses and breakouts using the Mohr-Coulomb failure criterion.

Lang et al. (2011) concluded that the workflow for wellbore stability modeling should consider bedding planes, rock anisotropy, and pressure depletion. With the consideration of these factors, the wellbore model enables the calculation of wellbore failures along borehole trajectories with various drilling orientations versus bedding directions. At the end of the study, they were able to develop a wellbore stability model and real-time surveillance for the drilling operations in the deep-water Gulf of Mexico. By applying this model and observing real-time updates, the drilled well reached target depths safely. It also decreased the drilling cost by 6 million dollars.

Soroush (2011) proposed a new workflow for the identification of borehole breakouts by processing eight chosen petrophysical logs in addition to mud weight and vertical stress. This process includes using the wavelet de-noising technique to remove noises from the original petrophysical logs and then using statistical classifiers (Parzen and Bayesian) to classify each depth into BO or nBO zones. This approach was applied to the data from five wells drilled in a carbonate reservoir. The results showed that, having good quality image data available at least in one interval or one well in the similar formation in a field, the Bayesian classifier is capable of identifying BO and nBO intervals with a reasonable accuracy of significantly higher than Parzen.

B. S. Aadnoy (2011) investigated typical wellbore fracturing and collapse models with respect to the accuracies in the input data. It was shown that the cumulative uncertainty is considerable. To reduce this uncertainty, constraints on the in-situ stress states are invoked. The need for model calibration was advocated. In addition to using leak-off, breakout and wellbore image data, methods such as establishing bounds on the in-situ data, data normalization and inversion methods are proposed to improve accuracy and to provide quality assurance.

Osisanya (2012) in his work on practical approach to solving wellbore instability problems came up with the following conclusions:

Before Drilling

1. Mechanical Earth Model must be utilized to predict wellbore instability problems in an upcoming well.

2. We must anticipate remedial actions to be used, which depend on type of instability and its severity.

While Drilling

3. We must employ the best drilling practices (e.g. reduction of surge/swab pressures and drillstring vibrations) as well as excellent mud chemistry.
4. ROP and hole cleaning efficiency form the key links between wellbore instability and operations. Hence, we must optimize hole cleaning and minimize open hole time.
5. Must perform continuous caving analysis and control surface parameters.

After Drilling

6. Perform Post-Drilling Review – collect data and update MEM); detail wellbore instability events.

Gholami et al. (2014) used Mohr-coulomb, Hoek-brown and Mogi-Coulomb failure criteria to estimate the potential rock failure around a wellbore located in an onshore field of Iran. The log based analysis was used to estimate rock mechanical properties of formations and state of stresses. The results indicated that amongst different failure criteria, the Mohr–Coulomb criterion underestimates the highest mud pressure required to avoid breakouts around the wellbore. It also predicts a lower fracture gradient pressure. In addition, it was found that the results obtained from Mogi–Coulomb criterion yield a better comparison with breakouts observed from the caliper logs than that of Hoek–Brown criterion. It was concluded that the Mogi–Coulomb criterion is a better

failure criterion as it considers the effect of the intermediate principal stress component in the failure analysis.

Udegbunam et al. (2014) investigated typical fracture and collapse models with respect to accuracies in the input data with a stochastic method. Uncertainties in the input data, which include in-situ stresses, rock strength data, and pore pressure were evaluated, to show how these contribute to the cumulative uncertainties in the model predictions. A fully probabilistic wellbore stability analyses was presented, with pre-exiting deterministic wellbore models as bases. The analyses was based on Monte Carlos forecast, whereby the model input parameters assume probability distributions. The MATLAB program was used for the analyses because its robustness and simplicity.

Al-Khayari, Al-Ajmi, and Al-Wahaibi (2016) presented a new probabilistic wellbore stability model to predict the critical drilling fluid pressure before the onset of a wellbore collapse. The model runs Monte Carlo simulation to capture the effects of uncertainty in in situ stresses, drilling trajectories, and rock properties. The developed model was applied to different in situ stress regimes: normal faulting, strike slip, and reverse faulting. Sensitivity analysis was applied to all carried out simulations and found that well trajectories have the biggest impact factor in wellbore instability followed by rock properties. The developed model improves risk management of wellbore stability.

Patel, Penkar, and Blyth (2018) presented an integrated approach to pore pressure prediction and managing drilling risk by incorporating multiple sources of information beyond classical log-based techniques. They demonstrated the value of advanced mud gas interpretation, drilling mechanics

interpretation, cavings and drilling parameter analysis to optimize the pore pressure model in real-time and enhance the traditional techniques.

2.10 BAYESIAN LEARNING

Bayesian learning methods are relevant to our study of machine learning for two different reasons. First, Bayesian learning algorithms that calculate explicit probabilities for hypotheses, such as the naive Bayes classifier, are among the most practical approaches to certain types of learning problems. For example, Michie, Spiegelhalter, and Taylor (1994) provide a detailed study comparing the naive Bayes classifier to other learning algorithms, including decision tree and neural network algorithms. These researchers show that the naive Bayes classifier is competitive with these other learning algorithms in many cases and that in some cases it outperforms these other methods (Mitchell, 1997).

2.10.1 Bayes Theorem

In machine learning we are often interested in determining the best hypothesis from some space H, given the observed training data D. One way to specify what we mean by the best hypothesis is to say that we demand the most probable hypothesis, given the data D plus any initial knowledge about the prior probabilities of the various hypotheses in H. Bayes theorem provides a direct method for calculating such probabilities. More precisely, Bayes theorem provides a way to calculate the probability of a hypothesis based on its prior probability, the probabilities of observing various data given the hypothesis, and the observed data itself (Mitchell, 1997).

Bayes theorem is the cornerstone of Bayesian learning methods because it provides a way to calculate the posterior probability P(h|D), from the prior probability P(h), together with P(D) and P(D|h).

Bayes theorem:

$$P(h|D) = \frac{P(D|h)P(h)}{P(D)} \quad (2.26)$$

As one might intuitively expect, P(h|D) increases with P(h) and with P(D|h) according to Bayes theorem. It is also reasonable to see that P(h|D) decreases as P(D) increases, because the more probable it is that D will be observed independent of h, the less evidence D provides in support of h.

2.10.2 Naïve Bayes Classifier

One highly practical Bayesian learning method is the naive Bayes learner, often called the naive Bayes classifier. In some domains its performance has been shown to be comparable to that of neural network and decision tree learning.

The naive Bayes classifier applies to learning tasks where each instance x is described by a conjunction of attribute values and where the target function f(x) can take on any value from some finite set V. A set of training examples of the target function is provided, and a new instance is presented, described by the tuple of attribute values (a_1, a_2 …a_n). The learner is asked to predict the target value, or classification, for this new instance (Mitchell, 1997).

Naive Bayes classifier:

$$v_{NB} = arg \max_{v_j \epsilon \forall} P(v_j) \prod_i P(a_i|v_j) \quad (2.27)$$

where V_{NB} denotes the target value output by the naive Bayes classifier.

One interesting difference between the naive Bayes learning method and other learning methods we have considered is that there is no explicit search through the space of possible hypotheses (in this case, the space of possible hypotheses is the space of possible values that can be assigned to the various $P(v_j)$ and $P(a_i|v_j)$ terms). Instead, the hypothesis is formed without searching, simply by counting the frequency of various data combinations within the training examples.

CHAPTER 3

METHODOLOGY

3.1 INTRODUCTION

In this chapter, a methodology which begins with the generation of synthetic data, adoption of specific failure models and culminating in the prediction of wellbore failure using Bayesian algorithm is adopted. Figure 3.1 shows the methodology adopted in this research. It includes the major elements of the work flow.

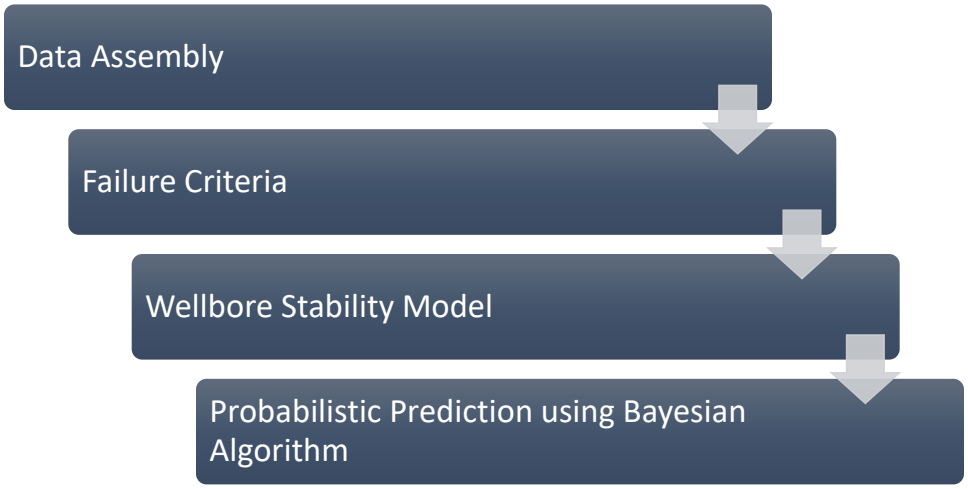

Figure 3. 1: **Research Methodology Workflow**

3.2 DATABASE ASSEMBLY

The data used in this study was synthetic data, so as to generate data sets that are flexible and rich enough to conduct machine learning in all its ramifications.

A total of 263 different sample sets were used, each with 7 major input parameters. Table 3.1 shows the minimum, maximum, mean and standard deviation of the data that was used.

Table 3. 1: **Data Statistics**

Parameter	Minimum	Maximum	Mean	Standard Deviation
σ_v (psi/ft)	0.908	0.976	0.942	0.0219
σ_H (psi/ft)	0.838	0.992	0.901	0.0502
σ_h (psi/ft)	0.788	0.942	0.851	0.0502
Pore pressue gradient (psi/ft)	0.450	0.905	0.537	0.154
Cohesion (psi)	710.69	2291.60	1294.53	464.28
Friction angle (deg.)	24.89	29.68	26.59	1.40
Poisson's ratio	0.25	0.25	0.25	0

3.3 FAILURE CRITERION DETERMINATION

These criteria are sets of functions in stress or strain spaces that describe or predict the condition at which rock fails under external load. In literature, many of failure criteria have been developed by scientists who suggested different approaches trying to simulate actual rock failures. In this paper, the concentration will be on Mogi-Coulomb criterion and Mohr-Coulomb criterion.

3.3.1 DETERMINATION OF BREAKOUT PRESSURE

For both criterions used, there are three different permutations of the three different stresses (σ_r, σ_z, and σ_θ). These permutations and their corresponding breakout pressure are shown in Table 2.2 and Table 2.7. Wellbore failure will occur if the well internal pressure is less than this breakout pressure. It has also been proven in literature that the most common stress distribution is the second case when $\sigma_\theta \geq \sigma_z \geq \sigma_r$, and this is called reverse faulting stress regime. Thus, this was the case used in this studies.

Mohr-Coulomb Criterion

$$\boldsymbol{P_{w(BO)}} = (A - C)/(1 + q) \quad (3.1)$$

Mogi-Coulomb Criterion

$$\boldsymbol{P_{w(BO)}} = \frac{1}{2}A - \frac{1}{6}\sqrt{12(a' + b'(A - 2P_o)^2 - 3(A - 2B)^2} \quad (3.2)$$

Where

$$A = 3\sigma_H - \sigma_h \quad (3.3)$$

$$B = \sigma_V + 2v(\sigma_H - \sigma_h) \quad (3.4)$$

$$C = C_o - P_o(q - 1) \quad (3.5)$$

$$q = tan^2(\pi/4 + \emptyset/2) \quad (3.6)$$

$$a' = 2c\cos\emptyset \quad (3.7)$$

$$b' = \sin\emptyset \quad (3.8)$$

3.3.2 DETERMINATION OF FRACTURE PRESSURE

There are also three different permutations of the three different stresses as illustrated for breakout pressure .These permutations and their corresponding fracture pressure are shown in Table 2.3 and Table 2.8. Wellbore failure will occur if the well internal pressure is greater than this fracture

pressure. Combination of the breakout pressure and fracture pressure defines our safe mud weight window, where breakout pressure is the lower bound and fracture pressure is the upper bound.

Mohr-Coulomb Criterion

$$\boldsymbol{P_{w(Frac)}} = C + qE \tag{3.9}$$

Mogi-Coulomb Criterion

$$\boldsymbol{P_{w(Frac)}} = \frac{1}{6-2b'^2}\left[(3D + 2b'N) + \sqrt{J + 12(N^2 + b'DN)}\right] \tag{3.10}$$

Where

$$D = 3\sigma_h - \sigma_H \tag{3.11}$$

$$E = \sigma_V - 2v(\sigma_H - \sigma_h) \tag{3.12}$$

$$J = D^2\left(4b'^2 - 3\right) + (E^2 - DE)\left(4b'^2 - 12\right) \tag{3.13}$$

$$N = a' + b'(E - 2P_o) \tag{3.14}$$

3.4 PREDICTION USING BAYESIAN ALGORITHM (GAUSSIAN NAÏVE BAYES)

Naive Bayes is a classification algorithm for binary (two-class) and multi-class classification problems. The technique is easiest to understand when described using binary or categorical input values.

Naive Bayes can be extended to real-valued attributes, most commonly by assuming a Gaussian distribution - This extension of naive Bayes is called Gaussian Naive Bayes (GNB), which was used in this studies.

3.4.1 DATA PROCESSING

Data for classification problems can very often be textual or non-numeric. In this case, the condition of the wellbore (stable/unstable) is non-numeric. GNB however cannot be trained with non-numeric. Hence, it was transformed to a numeric form.

There are several ways to translate textual or symbolic data into numeric data. Unary encoding, numbering classes and binary encoding are some of the common symbol translation techniques. Numbering classes is used in this study to perform symbol translation. Thus, for condition of the wellbore, numbers can represent the conditions namely stability=1, instability=0.

In this study, 70% of the datasets are used to train the classifier and the remaining 30% are used to test the classifier.

Table 3. 2: **Division of database**

Total Dataset=263	**Partition of Total**	**Number of Sample**
Training	70%	184
Testing	30%	79

3.4.2 WELLBORE FAILURE PREDICTION

Various libraries such as sklearn, pandas, numpy etc. were used to accomplish the end result of the project. The comparison result was based on precision, f1-score, recall and support of the confusion matrix. Confusion matrix is a matrix that gives the performance of the model as the output. The confusion matrix has four (4) major parameters namely;

- True Positive (TP) – These are the actual predicted true values of the classification. It simply means that the predicted class is 1 (yes) and the actual class is 1 (yes).
- True Negatives (TN) – These are the true predicted values that are negative. It simply means that the predicted class is 0 (no) and the actual class is 0 (no).
- False Positives (FP) – These are the values that are recorded as false instead of true. It simply means that the predicted class is 1 (yes) and the actual class is 0 (no).
- False Negatives (FN) – These are the values that are recorded as true instead of false. It simply means that the predicted class is 0 (no) and the actual class is 1 (yes).

In form of a matrix, the result of the confusion matrix takes this form

Table 3. 3: **Confusion Matrix**

	Predicted Class		
Actual Class		1 (yes)	0 (no)
	1 (yes)	True Positive (TP)	False Negative (FN)
	0 (no)	False Positive (FP)	True Negative (TN)

3.4.2.1 Precision

Precision has to do with the positive values in the matrix. It is the ratio of the correctly predicted value to the sum of the predicted positive values. It gives the result of the actual prediction returned by the classifier.

$$\text{Precision} = TP / (TP + FP) \quad (3.15)$$

3.4.2.2 Recall

Recall is also referred to as sensitivity. It is the ratio of the appropriately predicated positive value to the sum of the actual class 1 (yes). It gives the result of the actual labels to the true positive value. It also means the total percentage of the true positive values correctly classified

$$\text{Recall} = TP / (TP + FN) \quad (3.16)$$

3.4.2.3 F1 Score

F1 score takes into consideration both false positive values and false negative values. It is the weighted average of recall and precision by two (2). F1 reaches its best value at 1 and its worse at 0. It tells how precise the classifier is.

$$\text{F1 score} = 2 * (\text{Recall} * \text{Precision}) / (\text{Recall} + \text{Precision}) \quad (3.17)$$

3.4.2.4 Accuracy

Accuracy is one of the most vital results from the classifier. It is the ratio of the total predicted true values to the sum of the total interpretations on the matrix table. There is maximum output when there is equal number of samples belonging to the various categories

$$\text{Accuracy} = TP+TN \,/\, (TP+FP+FN+TN) \tag{3.18}$$

CHAPTER 4

RESULTS AND DISCUSSION

4.1 INTRODUCTION

In this study, Gaussian Naïve Bayes algorithm was applied to Mohr-Coulomb and Mogi-Coulomb failure criterion models to predict wellbore failure. Confusion matrix and plots of the results were generated to properly visualize and analyze the results discussed in the following sections.

4.2 CONFUSION MATRIX OF THE MOGI-COULOMB MODEL

As can been seen in Figure 4.1, The GNB algorithm gave 55 predictions as stable out of which 54 were actually stable and 24 predictions of unstable out of which 15 were actually unstable. The Bayesian algorithm showed a good capability in predicting the stable class (precision of 98%) and a fairly reasonable precision of 62% in predicting the unstable class. This yielded an overall accuracy of 87.3% which was a significant achievement.

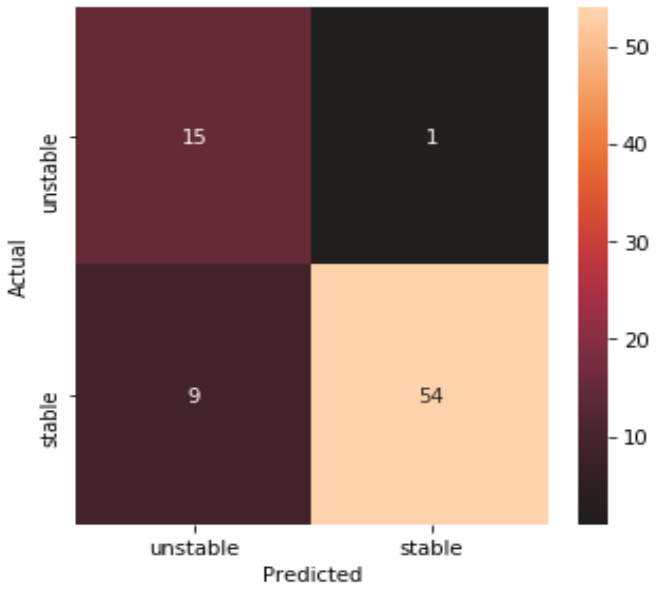

Figure 4. 1: **Mogi-Coulomb Confusion Matrix**

4.3 CONFUSION MATRIX OF THE MOHR-COULOMB MODEL

As can been seen in Figure 4.2, The GNB algorithm gave 42 predictions as stable out of which 24 were actually stable and 37 predictions of unstable out of which 28 were actually unstable. The Bayesian algorithm was not quite strong in predicting the stable class (precision of 57%) and a fairly reasonable precision of 76% in predicting the unstable class. This yielded an overall accuracy of 65.8% which was lesser than Mogi-Coulomb model but still quite reasonable.

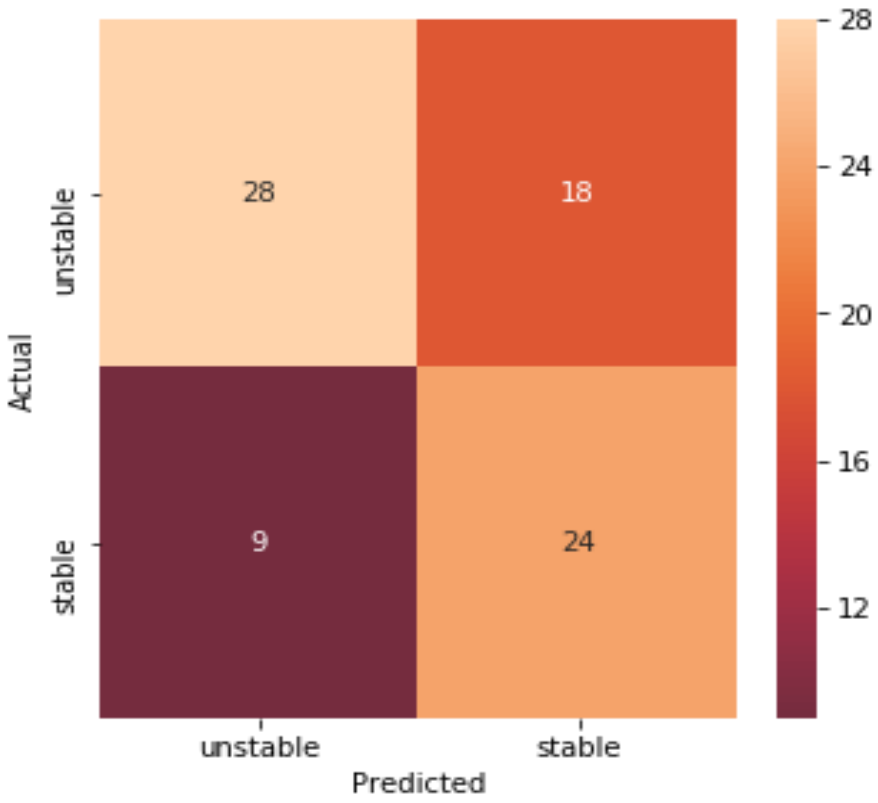

Figure 4. 2: **Mohr-Coulomb Confusion Matrix**

4.4 COMPARISON METRICS BETWEEN MOGI-COULOMB AND MOHR-COULOMB FAILURE CRITERION

In Figure 4.3, a comparison between Mogi-Coulomb and Mohr-Coulomb model using the accuracy, f1-score, recall and precision as the yardstick clearly showed that Mogi GNB outperformed Mohr GNB.

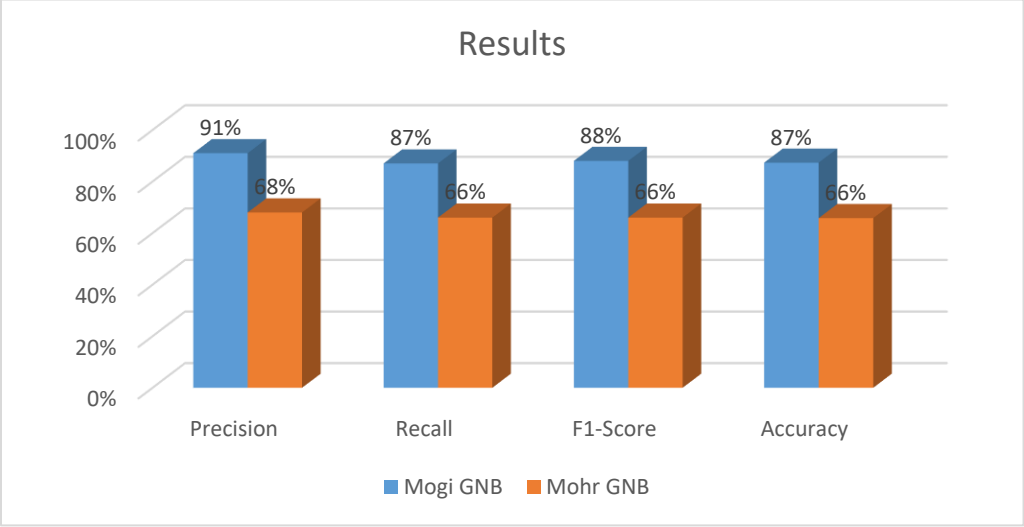

Figure 4. 3: **Comparison between Mogi Model and Mohr Model**

CHAPTER 5

CONCLUSIONS AND RECOMMENDATIONS

5.1 CONCLUSIONS

This study aimed to utilize machine learning in the prediction of wellbore failure. Two failure criterion models including Mogi-Coulomb failure criterion and Mohr-Coulomb failure criterion were employed for the determination of the safe mud weight window which was used with conjunction with our mud weight pressure to classify each depth into stable or unstable.

The Gaussian Naïve Bayes algorithm was successfully used to train and test the data set obtained after the application of each failure criterion models. The results showed that the Mogi-Coulomb model yielded a better prediction accuracy.

Therefore, this Bayesian model could be used as a wellbore stability management tool to predict wellbore failure. With a good knowledge of the controllable and uncontrollable factors influencing wellbore instability, possible precautionary measures could be taken to prevent or mitigate wellbore instability issues. Such important decisions could be:

- **Controllable Factors**
    1. Maintain efficient mud density, which is usually the most important determinant of stability in an open hole.
    2. Must perform continuous caving analysis and control surface parameters.
    3. Development of new drilling fluid systems that would mitigate fluid-rock interaction phenomena which modify the near-wellbore rock strength or stress.
    4. Optimization of the drill fluid temperature

5.2 RECOMMENDATIONS

This study was only carried out for vertical wellbore, which rarely seems to be the case in the field. Thus, the work should be adapted for inclined wellbore with different degrees of inclination and azimuth taken into consideration.

This study should also be extended to account for other physical phenomena such as chemical reactions and temperature. This will make the model more robust and relevant to the oil industry.

REFERENCES

1. Aadnoy, B., & Chenevert, M. (1987). Stability of highly inclined boreholes (includes associated papers 18596 and 18736). *SPE Drilling Engineering*, *2*(04), 364-374.

2. Aadnoy, B., Cooper, I., Miska, S., Mitchell, R. F., & Payne, M. L. (2009). *Advanced drilling and well technology*: SPE.

3. Aadnoy, B. S. (2011). *Quality assurance of wellbore stability analyses.* Paper presented at the SPE/IADC Drilling Conference and Exhibition.

4. Al-Ajmi, A. M., & Zimmerman, R. W. (2005). Relation between the Mogi and the Coulomb failure criteria. *International Journal of Rock Mechanics and Mining Sciences*, *42*(3), 431-439.

5. Al-Khayari, M. R., Al-Ajmi, A. M., & Al-Wahaibi, Y. (2016). Probabilistic Approach in Wellbore Stability Analysis during Drilling. *Journal of Petroleum Engineering*, *2016*, 13. doi:10.1155/2016/3472158

6. Bin Rabaa, A. S., Abass, H. H., Hembling, D. E., & Finkbeiner, T. (2007). *A Geomechanical Facies-Based Approach To Optimize Drilling and Completion Strategy of an Unconsolidated Sandstone Reservoir, Saudi Arabia*. Paper presented at the SPE Annual Technical Conference and Exhibition, Anaheim, California, U.S.A. https://doi.org/10.2118/109774-MS

7. Bowes, C., & Procter, R. (1997). Drillers stuck pipe handbook, 1997 guidelines & drillers handbook credits. *Schlumberger, Ballater, Scotland*.

8. Bradley, W. (1979). Failure of inclined boreholes. *Journal of Energy Resources Technology*, *101*(4), 232-239.

9. Chen, X., Tan, C. P., & Haberfield, C. M. (2002). A comprehensive, practical approach for wellbore instability management. *SPE Drilling & Completion*, *17*(04), 224-236.

10. Colmenares, L. B., & Zoback, M. D. (2002). A statistical evaluation of intact rock failure criteria constrained by polyaxial test data for five different rocks. *International Journal of Rock Mechanics and Mining Sciences*, *39*(6), 695-729. doi:https://doi.org/10.1016/S1365-1609(02)00048-5

11. Cui, L., Abousleiman, Y., Ekbote, S., Roegiers, J. C., & Zaman, M. (1999). *A Software for Poroelastic Analyses of Borehole Stability*. Paper presented at the Latin American and Caribbean Petroleum Engineering Conference, Caracas, Venezuela. https://doi.org/10.2118/54013-MS

12. de Fontoura, S. A., Holzberg, B. B., Teixeira, É. C., & Frydman, M. (2002). *Probabilistic analysis of wellbore stability during drilling.* Paper presented at the SPE/ISRM Rock Mechanics Conference.

13. Elijah, J. E. (2013). *NUMERICAL MODELING OF WELLBORE INSTABILITY (TENSILE FAILURE) USING FRACTURE MECHANICS APPROACH*. (Master of Science), African University of Science and technology, Abuja.

14. Fuh, G. F., Deom, D. B., & Turner, R. D. (1991). *Wellbore Stability and Drilling Results From the First Horizontal Well in the Kotter Field Offshore The Netherlands*. Paper presented at the SPE Annual Technical Conference and Exhibition, Dallas, Texas. https://doi.org/10.2118/22544-MS

15. Fung, L. S. K., Wan, R. G., Rodriguez, H., & Bellorin, I. R. S. (1996). *An Advanced Elasto-plastic Model For Borehole Stability Analysis of Horizontal Wells In Unconsolidated Formation*. Paper presented at the Annual Technical Meeting, Calgary, Alberta. https://doi.org/10.2118/96-58

16. Gaurina-Međimurec, N. (1998). Horizontal well drill-in fluids. *Rudarsko-geološko-naftni zbornik, 10*(1), 73-76.

17. Gholami, R., Moradzadeh, A., Rasouli, V., & Hanachi, J. (2014). Practical application of failure criteria in determining safe mud weight windows in drilling operations. *Journal of Rock Mechanics and Geotechnical Engineering, 6*(1), 13-25.

18. Gravley, W. (1983). Review of downhole measurement-while-drilling systems. *Journal of Petroleum Technology, 35*(08), 1,439-431,445.

19. Hawkes, C., & McLellan, P. (1999). A new model for predicting time-dependent failure of shales: theory and application. *Journal of Canadian Petroleum Technology, 38*(12).

20. Hoek, E., & Brown, E. (1980). Underground excavations in rock. Inst. *Mining and Metallurgy, London*, 156.

21. Jahanbakhshi, R., Keshavarzi, R., & Jahanbakhshi, R. (2012). *Intelligent Prediction of Wellbore Stability In Oil And Gas Wells: An Artificial Neural Network Approach*. Paper presented at the 46th U.S. Rock Mechanics/Geomechanics Symposium, Chicago, Illinois. https://doi.org/

22. Lang, J., Li, S., & Zhang, J. (2011). *Wellbore Stability Modeling And Real-Time Surveillance For Deepwater Drilling To Weak Bedding Planes And Depleted Reservoirs*. Paper presented at the SPE/IADC Drilling Conference and Exhibition, Amsterdam, The Netherlands. https://doi.org/10.2118/139708-MS

23. Li, S., & Purdy, C. C. (2010). *Maximum Horizontal Stress and Wellbore Stability While Drilling: Modeling and Case Study*. Paper presented at the SPE Latin American and Caribbean Petroleum Engineering Conference, Lima, Peru. https://doi.org/10.2118/139280-MS

24. Lowrey, J. P., & Ottesen, S. (1995). An assessment of the mechanical stability of wells offshore Nigeria. *SPE Drilling & Completion, 10*(01), 34-41.

25. McLellan, P. J. (1996). Assessing The Risk Of Wellbore Instability In Horizontal And Inclined Wells. *Journal of Canadian Petroleum Technology, 35*(05), 13. doi:10.2118/96-05-02

26. Michie, D., Spiegelhalter, D., & Taylor, C. (1994). Machine Learning, Neural and Statistical Classification.

27. Mitchell, T. M. (1997). *Machine Learning* (1st edition ed.). New York: McGraw-Hill.

28. Mody, F. K., Tare, U. A., & Wang, G. (2007). *Sustainable Deployment of Geomechanics Technology to Reducing Well Construction Costs*. Paper presented at the SPE/IADC Middle East Drilling and Technology Conference, Cairo, Egypt. https://doi.org/10.2118/108241-MS

29. Mogi, K. (1971). Fracture and flow of rocks under high triaxial compression. *Journal of Geophysical Research (1896-1977), 76*(5), 1255-1269. doi:10.1029/JB076i005p01255

30. Mohiuddin, M., Awal, M., Abdulraheem, A., & Khan, K. (2001). *A new diagnostic approach to identify the causes of borehole instability problems in an offshore Arabian field.* Paper presented at the SPE Middle East Oil Show.

31. Mohr, O. (1900). Welche Umstände bedingen die Elastizitätsgrenze und den Bruch eines Materials. *Zeitschrift des Vereins Deutscher Ingenieure, 46*(1524-1530), 1572-1577.

32. Morita, N. (2004). *Well Orientation Effect on Borehole Stability*. Paper presented at the SPE Annual Technical Conference and Exhibition, Houston, Texas. https://doi.org/10.2118/89896-MS

33. Nguyen, D. A., Miska, S. Z., Yu, M., & Saasen, A. (2010). *Modeling Thermal Effects on Wellbore Stability*. Paper presented at the Trinidad and Tobago Energy Resources Conference, Port of Spain, Trinidad. https://doi.org/10.2118/133428-MS

34. Nguyen, V. X., & Abousleiman, Y. N. (2009). *The Porochemothermoelastic Coupled Solutions of Stress and Pressure With Applications to Wellbore Stability in Chemically Active Shale*. Paper presented at the SPE Annual Technical Conference and Exhibition, New Orleans, Louisiana. https://doi.org/10.2118/124422-MS

35. Onaisi, A., Locane, J., & Razimbaud, A. (2000). *Stress related wellbore instability problems in deep wells in ABK field*. Paper presented at the Abu Dhabi International Petroleum Exhibition and Conference, Abu Dhabi, United Arab Emirates. https://doi.org/10.2118/87279-MS

36. Ong, S. H., & Roegiers, J. C. (1993). Influence of anisotropies in borehole stability. *International Journal of Rock Mechanics and Mining Sciences & Geomechanics Abstracts, 30*(7), 1069-1075. doi:https://doi.org/10.1016/0148-9062(93)90073-M

37. Osisanya, S. O. (2012). Practical approach to solving wellbore instability problems. *SPE Distinguished Lecture series, Port Harcourt*.

38. Ottesen, S. (2010). *Wellbore Stability in Fractured Rock*. Paper presented at the IADC/SPE Drilling Conference and Exhibition, New Orleans, Louisiana, USA. https://doi.org/10.2118/128728-MS

39. Pašić, B., Gaurina Međimurec, N., & Matanović, D. (2007). Wellbore instability: causes and consequences. *Rudarsko-geološko-naftni zbornik, 19*(1), 87-98.

40. Patel, N., Penkar, S., & Blyth, M. (2018). *Managing Drilling Risk Using an Integrated Approach to Real-Time Pore Pressure Prediction.* Paper presented at the Abu Dhabi International Petroleum Exhibition & Conference.

41. Sanchez D, M., Cabrera S, J. R., & Coll, C. (1996). *Geomechanical Design and Evaluation of a Horizontal Wellbore in Maracaibo Lake, Venezuela: Real-Drilling-Time Application*. Paper presented at the International Conference on Horizontal Well Technology, Calgary, Alberta, Canada. https://doi.org/10.2118/37088-MS

42. Santarelli, F. J., Dahen, D., Baroudi, H., & Sliman, K. B. (1992). Mechanisms of borehole instability in heavily fractured rock media. *International Journal of Rock Mechanics and Mining Sciences & Geomechanics Abstracts, 29*(5), 457-467. doi:https://doi.org/10.1016/0148-9062(92)92630-U

43. Santarelli, F. J., Zaho, S., Burrafato, G., Zausa, F., & Giacca, D. (1996). *Wellbore Stability Analysis Made Easy and Practical*. Paper presented at the SPE/IADC Drilling Conference, New Orleans, Louisiana. https://doi.org/10.2118/35105-MS

44. Simangunsong, R., Villatoro, J. J., & Davis, A. K. (2006). *Wellbore Stability Assessment for Highly Inclined Wells Using Limited Rock-Mechanics Data*. Paper presented at the SPE Annual Technical Conference and Exhibition, San Antonio, Texas, USA. https://doi.org/10.2118/99644-MS

45. Sinha, B. K., Wang, J., Kisra, S., Li, J., Pistre, V., Bratton, T., . . . Jun, C. (2008). *Estimation Of Formation Stresses Using Borehole Sonic Data*. Paper presented at the SPWLA 49th Annual Logging Symposium, Austin, Texas. https://doi.org/

46. Soreide, O. K., Bostrom, B., & Horsrud, P. (2009). *Borehole Stability Simulations of an HPHT Field Using Anisotropic Shale Modeling*. Paper presented at the 43rd U.S. Rock Mechanics Symposium & 4th U.S. - Canada Rock Mechanics Symposium, Asheville, North Carolina. https://doi.org/

47. Soroush, H. (2011). *Bayesian Algorithm Opens Way to Wellbore Stability*. Paper presented at the International Petroleum Technology Conference.

48. Tan, C., & Willoughby, D. (1993). *Critical mud weight and risk contour plots for designing inclined wells.* Paper presented at the SPE annual technical conference and exhibition.

49. Tran, M. H., & Abousleiman, Y. N. (2010). *The impacts of failure criteria and geological stress states on the sensitivity of parameters in wellbore stability analysis.* Paper presented

at the 44th US Rock Mechanics Symposium and 5th US-Canada Rock Mechanics Symposium.

50. Udegbunam, J. E., Aadnøy, B. S., & Fjelde, K. K. (2014). Uncertainty evaluation of wellbore stability model predictions. *Journal of Petroleum Science and Engineering*, *124*, 254-263.

51. Wessling, S., Bartetzko, A., Pei, J., & Dahl, T. (2012). *Automation in Wellbore Stability Workflows*. Paper presented at the SPE Intelligent Energy International, Utrecht, The Netherlands. https://doi.org/10.2118/149766-MS

52. Wong, S. W., Veeken, C. A. M., & Kenter, C. J. (1994). The Rock Mechanical Aspects of Drilling a North Sea Horizontal Well. *SPE Drilling & Completion*, *9*(01), 47-52. doi:10.2118/23040-PA

53. Yu, M., He, S., Chen, Y., Takach, N., LoPresti, P., Zhou, S., & Al-Khanferi, N. M. (2012). *A Distributed Microchip System for Subsurface Measurement*. Paper presented at the SPE Annual Technical Conference and Exhibition, San Antonio, Texas, USA. https://doi.org/10.2118/159583-MS

54. Zhang, J., & Roegiers, J. C. (2000). *Horizontal Borehole Stability in Naturally Fractured Reservoirs*. Paper presented at the SPE/CIM International Conference on Horizontal Well Technology, Calgary, Alberta, Canada. https://doi.org/10.2118/65513-MS

55. Zhang, L., Cao, P., & Radha, K. (2010). Evaluation of rock strength criteria for wellbore stability analysis. *International Journal of Rock Mechanics and Mining Sciences*, *47*(8), 1304-1316.

APPENDICES

APPENDIX A: Python Libraries used in the Prediction

In [1]:
```
#To import important libraries

import numpy as np
import pandas as pd
import matplotlib.pyplot as plt
import seaborn as sns
from sklearn.naive_bayes import GaussianNB
from sklearn.model_selection import train_test_split
```

APPENDIX B: Interface for data analysis for Mogi-Coulomb

In [3]:
```
#To display first 5 rows of our data
df.head(5)
```

Out[3]:

	Poisson_Ratio	Cohesion	Friction_Angle	SV	SH	Sh	Po	Wellbore_Stability
0	0.25	884.73	25.38	7481.92	6905.12	6493.12	3708.0	1
1	0.25	884.73	25.38	7491.00	6913.50	6501.00	3712.5	1
2	0.25	884.73	25.38	7500.08	6921.88	6508.88	3717.0	1
3	0.25	884.73	25.38	7509.16	6930.26	6516.76	3721.5	1
4	0.25	884.73	25.38	7518.24	6938.64	6524.64	3726.0	1

In [4]:
```
df.describe()
```

Out[4]:

	Poisson_Ratio	Cohesion	Friction_Angle	SV	SH	Sh	Po	Wellbore_Stability
count	263.00	263.000000	263.000000	263.000000	263.000000	263.000000	263.000000	263.000000
mean	0.25	1294.534068	26.592776	11669.296008	11243.591103	10627.238821	6958.141217	0.794677
std	0.00	465.162432	1.397564	2963.149129	3223.249347	3080.770145	3634.934629	0.404708
min	0.25	710.690000	24.890000	7481.920000	6905.120000	6493.120000	3708.000000	0.000000
25%	0.25	884.730000	25.380000	9034.325000	8378.530000	7889.130000	4404.600000	1.000000
50%	0.25	1276.330000	26.480000	10588.760000	9908.540000	9341.690000	5101.650000	1.000000
75%	0.25	1783.970000	28.050000	14338.610000	14085.225000	13339.975000	7303.450000	1.000000
max	0.25	2291.600000	29.680000	16667.150000	16940.380000	16086.530000	15270.970000	1.000000

APPENDIX C: Implementing Naïve Bayes for Mogi-Coulomb

In [9]:
```
x_train,x_test,y_train,y_test=train_test_split(x,y,test_size=0.3,random_state=0)
```

In [10]:
```
from sklearn.naive_bayes import GaussianNB
nb=GaussianNB()
nb.fit(x_train,y_train)
print("Accuracy of Naive Bayes: {:.2f}%".format(nb.score(x_test,y_test)*100))
```

```
Accuracy of Naive Bayes: 87.34%
```

APPENDIX D: Confusion matrix for Mogi-Coulomb

Confusion Matrix

In [32]:
```
y_pred=nb.predict(x_test)
```

In [33]:
```
from sklearn.metrics import precision_score,recall_score,f1_score,confusion_matrix
```

In [34]:
```
confusion_matrix(y_test,y_pred)
```

Out[34]:
```
array([[15,  1],
       [ 9, 54]], dtype=int64)
```

In [37]:
```
from sklearn import metrics
from sklearn.metrics import classification_report
print('accuracy %s' %metrics.accuracy_score(y_test,y_pred))
print(classification_report(y_test,y_pred))
```

```
accuracy 0.8734177215189873
             precision    recall  f1-score   support

          0       0.62      0.94      0.75        16
          1       0.98      0.86      0.92        63

avg / total       0.91      0.87      0.88        79
```

APPENDIX E: Interface for data analysis for Mohr-Coulomb

In [3]:
```
#To display first 5 rows of our data
df.head(5)
```

Out[3]:

	Poisson_Ratio	Cohesion	Friction_Angle	SV	SH	Sh	Po	Wellbore_Stability
0	0.25	884.73	25.38	7481.92	6905.12	6493.12	3708.0	1
1	0.25	884.73	25.38	7491.00	6913.50	6501.00	3712.5	1
2	0.25	884.73	25.38	7500.08	6921.88	6508.88	3717.0	1
3	0.25	884.73	25.38	7509.16	6930.26	6516.76	3721.5	1
4	0.25	884.73	25.38	7518.24	6938.64	6524.64	3726.0	1

In [4]:
```
df.describe()
```

Out[4]:

	Poisson_Ratio	Cohesion	Friction_Angle	SV	SH	Sh	Po	Wellbore_Stability
count	263.00	263.000000	263.000000	263.000000	263.000000	263.000000	263.000000	263.000000
mean	0.25	1294.534068	26.592776	11669.296008	11243.591103	10627.238821	6958.141217	0.418251
std	0.00	465.162432	1.397564	2963.149129	3223.249347	3080.770145	3634.934629	0.494212
min	0.25	710.690000	24.890000	7481.920000	6905.120000	6493.120000	3708.000000	0.000000
25%	0.25	884.730000	25.380000	9034.325000	8378.530000	7889.130000	4404.600000	0.000000
50%	0.25	1276.330000	26.480000	10588.760000	9908.540000	9341.690000	5101.650000	0.000000
75%	0.25	1783.970000	28.050000	14338.610000	14085.225000	13339.975000	7303.450000	1.000000
max	0.25	2291.600000	29.680000	16667.150000	16940.380000	16086.530000	15270.970000	1.000000

APPENDIX F: Implementing Naïve Bayes for Mohr-Coulomb

In [9]:
```
x_train,x_test,y_train,y_test=train_test_split(x,y,test_size=0.3,random_state=0)
```

In [10]:
```
from sklearn.naive_bayes import GaussianNB
nb=GaussianNB()
nb.fit(x_train,y_train)
print("Accuracy of Naive Bayes: {:.2f}%".format(nb.score(x_test,y_test)*100))
```

```
Accuracy of Naive Bayes: 65.82%
```

APPENDIX G: Confusion matrix for Mohr-Coulomb

Confusion Matrix

In [13]:
```
y_pred=nb.predict(x_test)
```

In [14]:
```
Wellbore_Stability = ['unstable', 'stable']
```

In [15]:
```
from sklearn.metrics import precision_score,recall_score,f1_score,confusion_matrix
```

In [16]:
```
confusion_matrix(y_test,y_pred)
```

Out[16]:
```
array([[28, 18],
       [ 9, 24]], dtype=int64)
```

In [17]:
```
from sklearn import metrics
from sklearn.metrics import classification_report
print('accuracy %s' %metrics.accuracy_score(y_test,y_pred))
print(classification_report(y_test,y_pred))
```

```
accuracy 0.6582278481012658
             precision    recall  f1-score   support

          0       0.76      0.61      0.67        46
          1       0.57      0.73      0.64        33

avg / total       0.68      0.66      0.66        79
```